

Spatial structure of the globular cluster system and the distance to the galactic center

William E. Harris*

Yale University Observatory, New Haven, Connecticut

(Received 20 February 1976; revised 14 September 1976)

A new and comprehensive list of distance moduli for a total of 111 globular clusters is derived, following a re-evaluation of several methods of distance determination. For two-thirds of these clusters the distances can now be estimated directly from color-magnitude diagrams. The new distance list is used to obtain the centroid of the cluster system and hence an estimate for R_0 , the distance to the galactic center. The list is next used to derive the basic structural properties of the globular cluster system as a whole. The overall density distribution $\varphi(r)$ of the cluster system as a function of r (galacto-centric distance) is shown to follow closely a power law of the form $\varphi \sim r^{-3.5 \pm 0.5}$, over virtually the entire range of the halo ($3 \lesssim r \lesssim 30$ kpc). The space density distributions are also derived for low-, intermediate-, and high-metallicity subgroups, with the conclusion that all types of globular clusters are very strongly concentrated toward the galactic center and that all subgroups within the system can be approximated satisfactorily by a spherically symmetric distribution. The relation of the outermost halo objects (dwarf spheroidal systems and distant Palomar clusters) to the normal cluster system is briefly discussed. Finally, a rough estimate for the total mass of the halo, M_h , is derived, by assuming that the distribution of mass in the entire halo is similar to that in the globular cluster system.

INTRODUCTION

THE distance to the galactic center, R_0 , is one of the fundamental parameters in observational astronomy. Its importance to our understanding of the scale and structure of the Galaxy, and the well-known difficulty of measuring it accurately, imply that every available method for its determination should be pursued. One of the classic techniques for estimating R_0 comes from the simple assumption that the center of the Galaxy lies at the centroid of the system of globular clusters: This hypothesis was first used in a remarkable paper by Shapley (1918) to calculate R_0 and the overall size of the Galaxy. Since then, from time to time Shapley's method has been revised by other authors, the most recent treatments being by Fernie (1962) and Arp (1965a).

A related problem is the determination of the overall structure of the system of globular clusters. The general assumption is often made that the space distribution of the globular clusters represents the distribution of mass in the galactic halo as a whole. If this is true, then such features as the size, space density, and ellipticity of the cluster system will also describe the halo itself, aside from scale factors to correct for the relative total masses contained in the cluster system and the entire halo. Of all Population II objects, the globular clusters are by far the easiest to detect and measure at all distances from the Sun; thus, they provide a uniquely powerful method for explicitly measuring the structure of the halo.

An excellent opportunity to investigate these problems once again has now arisen, as the result of two major improvements in the fundamental data available for globular clusters. First, the measurement of literally dozens of new color-magnitude (CM) diagrams in the

past decade (see Table II) has greatly increased the number of clusters for which reliable distance estimates can be made. Second, the estimates of foreground reddnings for almost all the clusters are now available on an accurate and homogeneous system based on combining the clusters' integrated colors and spectral types to obtain E_{B-V} (Racine 1973, 1976; Burstein and McDonald 1975; Harris and van den Bergh 1974; van den Bergh 1967a). These advances allow a new compilation of cluster distances that is significantly more comprehensive and reliable than any previous list.

The aims of this paper are, first, to derive a new compilation of cluster distances on a homogeneous system that will be of general usefulness (Sects. I and II); second, to use the compiled data to calculate R_0 by Shapley's method (Sects. III and IV); and third, to discuss certain basic properties of the cluster system as a whole, including its overall size and density distribution and the relation between cluster metallicity and space distribution (Sects. V, VI, and VII). The latter sections lead into a brief discussion of the relation of the cluster system to the galactic halo in general, and a new estimate for the halo mass (Sect. VIII). [Recently Woltjer (1975) has published a shorter discussion of some similar topics. Although many of his conclusions resemble the ones presented here in areas where the material overlaps, the present discussion is based on a greatly improved and up-to-date sample of color-magnitude and reddening data, and is intended to provide a more thorough analysis of the methods involved and possible errors in the results.]

Considerably more information about the cluster system (its kinematics and orbital properties) may be obtained once the cluster radial velocities are introduced (e.g., Kinman 1959b; Arp 1965a; Woltjer 1975). However, a discussion of these topics is beyond the scope of this paper and would probably be premature in view of

* Present address: McMaster University, Department of Physics, Hamilton, Ontario, L8S 4M1 Canada.

the work in progress by other astronomers to obtain more accurate radial velocity measurements for many clusters.

I. METHODS FOR ESTIMATING CLUSTER DISTANCES

The first necessary step is the derivation of intrinsic distance moduli for as complete a list of clusters as possible. Estimating distances to globular clusters by photometry of their individual stars dates back more than 60 years (Shapley 1918, 1930; Sawyer Hogg 1959) yet still no completely satisfactory approach exists. The most fundamental method of distance determination currently available is through main-sequence fitting (cf. Sandage 1970; Hartwick and Hesser 1974), but main-sequence photometry is currently available for less than a dozen globular clusters. For the vast majority of the remaining objects, this approach remains prohibitive or impossible by present techniques and thus must still be used only to calibrate other distance indicators.

The methods for distance determination employed here are evaluated in the following subsections. The only techniques considered are those which, in some form or other, involve photometry of the individual cluster stars—that is, methods which refer to some identifiable luminosity level in the cluster's CM diagram—or measurement of the cluster luminosity as a whole. Several such techniques (described below in approximate order of decreasing precision) are available that are capable of estimating distance moduli to $\lesssim \pm 0.^m5$. Although some of these methods are useful only on a relatively crude level, they must occasionally be used of necessity to obtain any distance estimates at all for certain clusters. Fortunately, because of the large amount of new observational work now available, distance moduli for the majority of the known globular clusters can now be compiled with a new level of precision ($\sim \pm 0.^m1$).

A. The Horizontal Branch

By far the most reliable distance standard that can be applied in a widespread way is the level of the horizontal branch at the RR Lyrae region in the CM diagram. The problem of what absolute magnitude to apply to the horizontal branch (HB) has created one of the longest and most consistently active discussions in the astronomical literature. During the past decade, values near $M_V(HB) = 0.5$ have usually been used. An important step toward what seemed to be a solution was made by Christy (1966), who proposed, on the basis of a large set of pulsation models for RR Lyrae stars, that the "transition period" between the a- and c-type RR Lyrae stars in a cluster could be used to set the value of $M_V(HB)$. This in turn implied that $M_V(HB)$ should be expected to vary by up to $\sim 0.^m5$ from cluster to cluster, such that the more metal-rich clusters would have fainter horizontal branches. His procedure has been applied by several authors, notably Dickens (1970), Sandage (1970), and Kukarkin (1974). However, Christy's

TABLE I. Absolute magnitude of the horizontal branch.

(1) Main-sequence fitting of globular clusters		
Reference	Cluster	$M_V(HB)$
Sandage 1970	NGC 5272	0.57
Sandage 1970	6205	0.43
Sandage 1970	6341	0.92
Sandage 1970	7078	0.62
Hartwick and Vanden Berg 1973	6838	0.35
Hartwick and Hesser 1974	104	0.98
	Mean	0.65
		± 0.10
(2) Statistical parallax of field RR Lyrae stars		
Reference		$M_V(RR)$
van Herk 1965		0.68 ± 0.22
Woolley and Savage 1971		0.6 ± 0.2
Heck 1973		0.51 ± 0.20
Hemenway 1975		0.5 ± 0.4
(3) RR Lyrae stars in Magellanic Clouds		
Reference		$M_V(RR)$
Graham 1973, 1975		0.6 ± 0.2

method has been seriously challenged by several other writers (Iben 1971; Stobie 1971; van Albada and Baker 1973; Breger and Bregman 1975). Thus, it seems that any decisions about $M_V(HB)$ on strictly *theoretical* grounds must still await further work.

Observationally, $M_V(HB)$ may be calibrated in several ways. Table I summarizes recent results from three of the most important methods: main-sequence fitting from certain nearby globular clusters, statistical parallax of field RR Lyrae variables, and the RR Lyrae stars in the Magellanic Clouds. For the first method (main-sequence fitting), the value of $M_V(HB)$ is defined here as the level of the horizontal branch at the blue edge of the RR Lyrae gap. For the four clusters in Table I measured by Sandage (1970), the distance moduli listed are those resulting from his own observational fitting procedure, not the moduli he adopted from Christy's method. The average $M_V(HB)$ for all six clusters listed is 0.65 with a purely formal standard error of ± 0.1 . The new main-sequence data for 47 Tuc (Hartwick and Hesser 1974) provide the first strong observational support of Christy's result that $M_V(HB)$ should be fainter for the metal-rich clusters. Contrarily, the values for Sandage's four clusters indicate just the opposite trend. It should be stressed that $M_V(HB)$ determined for any one cluster can be uncertain by ± 0.4 or more: As discussed more extensively by Sandage, the calibration for the main sequence as a function of abundance is still in doubt, and quite tiny errors ($\lesssim 0.^m05$) in the adopted cluster reddenings or the observed colors of the faint main-sequence stars are reflected enormously in the magnitudes since the slope of the main sequence is $\Delta V / \Delta(B - V) \simeq 6$. In conclusion, the precise relation between $M_V(HB)$ and cluster metallicity still appears to be poorly defined. The choice made here is to adopt a single value for $M_V(HB)$ and apply it uniformly to every cluster.

The approach of using the RR Lyrae variables in the Magellanic Clouds to estimate $M_V(RR)$ is potentially powerful, since the Clouds present the only available opportunity to compare the RR Lyrae stars directly with the fundamental Population I cepheids. Graham (1973, 1975) states that the Cloud RR Lyrae stars show only a small ($\pm 0.^m2$) dispersion in absolute magnitude, in contrast to the main-sequence results for the galactic globular clusters. This conclusion is a strong one if the Cloud RR Lyrae stars are strictly comparable to those in the Galaxy.

The overall mean result from all three methods listed in Table I is $M_V(HB) = 0.6 \pm 0.3$, where the quoted error is a "realistic" estimate of the true uncertainty. The belief that this value should cover the observed cases is encouraged by the close agreement among the three (independent) methods, despite the well-known internal difficulties of each.

The level of the horizontal branch V_{HB} is adopted for this discussion as the fundamental distance indicator. The distance modulus of each cluster is thus given by

$$(m - M)_V = V_{HB} - 0.6. \quad (1)$$

Enough CM diagrams are now available that this approach can be used directly for 74 objects, almost two-thirds of the known globular clusters. For 37 of the remaining clusters, we may resort to a variety of secondary methods which are calibrated in terms of the primary horizontal-branch method. These are evaluated below.

B. 25 Brightest Stars

Shapley (1918) first began to estimate distances to the globular clusters by assuming a standard luminosity for the brightest stars in each cluster. To do this, he introduced the use of the mean photographic magnitude of the 25 brightest cluster stars, denoted here as $\langle m_{pg} \rangle_{25}$. For several clusters this is still the best available method. The difficulty with Shapley's straightforward approach is that no single absolute magnitude for $\langle m_{pg} \rangle_{25}$ can legitimately be applied to all clusters, since the modern CM studies revealed that the height of the brightest cluster giants above the horizontal branch should depend on both the cluster's total population and its heavy-element abundance (e.g., Sandage and Wallerstein 1960; Arp 1965a). The problem here is therefore to calibrate the height of $\langle m_{pg} \rangle_{25}$ above the horizontal branch as a function of cluster population and metallicity.

The published values of $\langle m_{pg} \rangle_{25}$ have been converted to $\langle B \rangle_{25}$ on the UBV system by Arp (1965a). First, we may define the "height" of $\langle B \rangle_{25}$ above the horizontal branch as

$$\delta B_{25} = B_{HB} - \langle B \rangle_{25}, \quad (2)$$

where

$$B_{HB} = V_{HB} + 0.17 + E_{B-V}. \quad (3)$$

Here V_{HB} denotes the level of the horizontal branch, as

before, at the blue edge of the RR Lyrae gap. The intrinsic color of the blue edge is taken as $(B - V)_0 = 0.17$ (Sandage 1969).

To a first approximation the total stellar population of a cluster can be represented by its absolute integrated magnitude,

$$M_{V_t} = V_t - (m - M)_V, \quad (4)$$

where V_t is its apparent integrated magnitude. Similarly, the metallicity can be represented by its integrated color $(B - V)_0$ or spectral type (Racine 1973, 1975; Burstein and McDonald 1975). Functionally, our hypothesis then becomes $\delta B_{25} = f[M_{V_t}, (B - V)_0]$.

The calibration of δB_{25} in terms of M_{V_t} and $(B - V)_0$ is carried out simply by using all 70 clusters for which CM diagrams and integrated magnitudes and colors are available. For these calibrating clusters, δB_{25} and $(m - M)_V$ are obtained directly from the CM diagrams, while $(B - V)_0$ and V_t are taken from published compilations (Racine 1976; Burstein and McDonald 1975; Peterson and King 1975; Harris 1974). The resulting two-parameter solution for δB_{25} is

$$\delta B_{25} = -0.12 - 0.14 M_{V_t} - 1.57 [(B - V)_0 - 0.70]. \quad (5)$$

This calibrating relation reproduces the defining points with an rms scatter of $\pm 0.^m3$ in δB_{25} . (This represents the internal error inherent in the method.)

This relation may now be combined with Eqs. (1)–(4) to yield an expression for V_{HB} in terms of directly observable quantities:

$$V_{HB} = 0.87 \{ \langle B \rangle_{25} - 0.14 V_t - 1.57 [(B - V)_0 - 0.70] - E_{B-V} - 1.15 \}. \quad (6)$$

Although this formula will predict V_{HB} with an internal standard error of $\sim \pm 0.^m3$ as in Eq. (5), the actual (external) random error is near $\pm 0.^m5$. This is because additional uncertainties are introduced when $\langle m_{pg} \rangle_{25}$ is transformed to $\langle B \rangle_{25}$. The original $\langle m_{pg} \rangle_{25}$ values were based on photometric scales of differing accuracy and do not form a homogeneous set of data (cf. the discussion by Arp 1965a). Thus, the primary source of uncertainty at present is within the old photographic data themselves. The method could be considerably improved if the brightest stars in a large number of clusters were re-measured on the UBV system.

Equation (6) may be used for any cluster for which V_t and $(B - V)_0$ are available. The overall mean value of δB_{25} for all the calibrating clusters is $\langle \delta B_{25} \rangle = 1.02 \pm 0.06$ (s.e.), and for clusters with no measured integrated magnitudes or colors the only recourse is to add $\langle \delta B_{25} \rangle$ directly to $\langle B \rangle_{25}$ to obtain B_{HB} .

C. Photographic Measurements of RR Lyrae Variables

The extensive body of data for globular clusters on the old m_{pg} system contains not only the photometry of the

brightest stars but also measurements of the RR Lyrae variables in dozens of clusters. The mean photographic magnitude of these variables, denoted here as $\langle m_{pg} \rangle_{RR}$, gives a direct estimate of the horizontal-branch level and hence the distance modulus of a cluster. This method is again an approximate one, giving $(m - M)_V$ to about the same accuracy as with the previous method ($\pm 0.^m 5$). Both of these techniques are subject to accidental magnitude errors of roughly this amount, first because the old photographic photometry was usually calibrated by photographic transfers to standard regions like the Selected Areas and North Polar Sequence, and second because further random scale errors may enter when m_{pg} is transformed into B .

All the relevant photographic data for the RR Lyrae cluster variables have been collected by Sawyer Hogg (1973). From this listing the mean magnitudes $\langle m_{pg} \rangle_{RR}$ can be directly obtained for every cluster with measured RR Lyrae variables but without any available CM diagram. The values of $\langle m_{pg} \rangle_{RR}$ are then transformed to $\langle B \rangle_{RR}$ with the scale relation given by Arp (1965a). These values of $\langle B \rangle_{RR} \simeq B_{HB}$ finally led to the desired estimates for $(m - M)_V$ through Eqs. (1) and (3).

D. Cluster Luminosities

Recently Kukarkin (1971, 1974) showed that the absolute integrated magnitude M_{V_t} of a globular cluster could be correlated with its "richness index" IR, which in turn is obtained directly from inspection of photographic plates. The distance modulus for any cluster with a measured integrated magnitude V_t can then be found by using its IR value to predict M_{V_t} . The distance follows from $(m - M)_V = V_t - M_{V_t}$.

The calibration of M_{V_t} vs IR is carried out by using the clusters in the "primary" distance modulus list, i.e., those with CM diagrams. Integrated magnitudes for most of these are available from other compilations (Peterson and King 1975; Harris 1974), and the IR values are taken from Kukarkin (1974). For 70 such clusters with both M_{V_t} and IR known, the best-fitting relation is

$$M_{V_t} = -6.94 \text{ IR} - 4.03 \quad (\pm 0.^m 6 \text{ s.e.}) \quad (7)$$

No significant correlations of the residuals about this mean line with cluster metallicity were found. Equation (7) differs slightly from the corresponding relation determined by Kukarkin [1974; see his Eq. (103)] principally because his fundamental distance scale $M_V(HB)$ differs from the one used here.

E. Visual Resolution of Cluster Stars

Van den Bergh (1967b) showed that distance estimates for a large number of clusters could be obtained simply by visual inspection of how well resolved they appeared to be when inspected through a small telescope.

This approach, though apparently rudimentary, is included here for completeness and because for a handful of clusters no better data are yet available.

Van den Bergh first placed the "degree of resolution" (DR) of the clusters on a quantitative scale, and then demonstrated that this parameter was well correlated with V_0 , the apparent V magnitude of the brightest cluster giants including atmospheric extinction. However, his calibration of DR vs V_0 depended on only 15 clusters with CM diagrams then available. The calibration can be redone here more reliably with the far larger number of CM diagrams. For 52 clusters in common with van den Bergh's list that have CM diagrams (Table II), the calibration becomes

$$V_0 = 15.8 - 1.0 \text{ DR} \quad (\pm 0.^m 5 \text{ s.e.}) \quad (8)$$

This is only slightly different from van den Bergh's original calibration. Despite its apparently simplistic approach, this method nevertheless yields distance estimates accurate at roughly the half-magnitude level.

V_0 as determined from Eq. (8) may now be used to predict V_{HB} . Following van den Bergh's procedure, V_0 is first corrected for atmospheric extinction to yield V_G , the level of the brightest cluster giants. Next, just as for the 25-brightest-stars technique, the height of these giants above the horizontal branch can be calibrated in terms of cluster metallicity [represented by $(B - V)_0$] and population (represented by M_{V_t}). For the 52 calibrating clusters the resulting relation is

$$\delta V = 1.97 - 0.08 M_{V_t} - 2.94 [(B - V)_0 - 0.70], \quad (9)$$

where $\delta V = V_{HB} - V_G$.

Finally, Eq. (9) is combined with Eqs. (1) and (4) to produce the desired expression for V_{HB} , in terms of V_G , $(B - V)_0$, and V_t ,

$$V_{HB} = 1.09 \{1.92 + V_G - 0.08 V_t - 2.94 [(B - V)_0 - 0.7]\}. \quad (10)$$

II. FINAL LIST OF DISTANCE MODULI

The methods discussed above have been used to compile the list of distance moduli presented in Table II. For any cluster with an available CM diagram (the "primary" method), the distance modulus obtained from it was accepted directly without averaging in any of the results from the secondary methods. A search of the literature yielded a total of 74 clusters with measured CM diagrams, the references for which are listed in the last column of Table II. These were used directly with the uniform assumption $M_V(HB) = 0.6$ as in Eq. (1) to determine $(m - M)_V$. For two clusters (NGC 6101, 6517) the available CM diagrams do not reach the horizontal branch; instead, their giant branches were fitted to those of comparison clusters (M3, M13) to estimate V_{HB} . The V_{HB} values as taken from the CM diagrams are expected to be accurate to $\lesssim \pm 0.^m 2$ in virtually all cases, although for all but the very best studied

GLOBULAR CLUSTER SYSTEM

1099

TABLE II. Distance moduli for 111 globular clusters.

NGC	Sp.T.	E_{B-V}	$(m - M)_V$	Method	Source
104 (47 Tuc)	G3	0.04	13.46	1	Hartwick and Hesser 1974
288	(F-)	0.00	14.70	1	Cannon 1974
362	(F8)	0.04	14.90	1	Menzies 1967
1261	F8	0.02	15.70	1	Alcaino and Contreras 1971
Pal 1	(F-)	0.12 ^a	18.7	3	
1851	F7	0.07	15.40	1	Alcaino 1971b
1904 (M79)	F6	0.00	15.65	1	Stetson and Harris 1976
2298	F7	0.11	15.80	1	Alcaino 1974a
2419	F5	0.03 ^b	19.94	1	Racine and Harris 1975
2808	F8	0.21	15.52	1	Harris 1975
Pal 3	(F-)	0.03 ^a	20.0	1	Burbidge and Sandage 1958
3201	(F+)	0.28	14.15	1	Menzies 1967
Pal 4	(F-)	0.00 ^a	19.85	1	Burbidge and Sandage 1958
4147	F2	0.02	16.28	1	Sandage and Walker 1955
4372	(F-)	0.45 ^b	14.90	1	Hartwick and Hesser 1973
4590 (M68)	F2	0.03 ^b	15.01	1	Harris 1975
4833	(F-)	0.38	14.90	1	Menzies 1972
5024 (M53)	F4	0.05	16.34	1	Cuffey 1965
5053	(F-)	0.03	16.00	1	Walker <i>et al.</i> 1976
5139 (ω Cen)	F7	0.11	13.92	1	Dickens and Saunders 1965
5272 (M3)	F7	0.00 ^b	15.00	1	Sandage 1970
5286	F8	0.27 ^b	15.61	1	Harris <i>et al.</i> 1976
5466	(F-)	0.05	15.96	1	Cuffey 1961
5634	F5	0.07	16.90	1	Racine 1974
5694	F3	0.08	17.60	1	Harris 1975
IC4499	(F+)	0.24	17.12	1	Fourcade <i>et al.</i> 1974
5824	F5	0.14	17.32	1	Harris 1975
Pal 5	(F-)	0.02 ^a	17.2	1,3,4	Kinman and Rosino 1962
5897	F5	0.06 ^a	15.60	1	Sandage and Karem 1968
5904 (M5)	F5	0.07	14.51	1	Arp 1962
5927	G2	0.55 ^b	16.10	1	Menzies 1974b
5946	(F+)	0.56	16.7:	5,6	
5986	F8	0.27	15.90	1	Harris <i>et al.</i> 1976
6093 (M80)	F7	0.21	15.28	1	Harris and Racine 1974
6101	(F-)	0.08	15.70	2	Alcaino 1974b
6121 (M4)	F8	0.31	12.90	1	Eggen 1972
6139	F8	0.68	17.0:	5,6	
6144	(F+)	0.36	15.6	3,4	
6171	G0-G1	0.37	15.03	1	Dickens and Rolland 1972
6205 (M13)	F5	0.02 ^b	14.35	1	Sandage 1970
6218 (M12)	F6	0.19	14.30	1	Racine 1971
6229	F7	0.01	17.2	3,4,5	
6235	(F+)	0.38	16.6	3,4,5	
6254 (M10)	F8	0.26 ^b	14.05	1	Harris <i>et al.</i> 1976
6266 (M62)	F8	0.46	15.38	1	Harris 1975
6273 (M19)	F4	0.38	16.35	1	Harris <i>et al.</i> 1976
6284	F9	0.27	16.0	3,4,6	
6287	G4	0.36	15.8	3,4,6	
6293	F3	0.34	15.5	3,4,6	
6304	G2	0.58 ^b	15.50	1	Hesser and Hartwick 1976b
6316	G4	0.48	16.7:	5,6	
6325	(F+)	0.80	16.70	1	Harris 1975
6333 (M9)	F3-F4	0.36	15.7	3,4	
6341 (M92)	F2	0.01 ^b	14.50	1	Sandage 1970
6342	G4	0.49	17.5:	5,6	
6352	(G)	0.25 ^b	14.47	1	Hartwick and Hesser 1972
6355	(G)	0.76	16.6:	5,6	
6356	G5	0.21	17.07	1	Sandage and Wallerstein 1960
6362	(F+)	0.12	14.65	1	Alcaino 1972
6366	(G)	0.65	15.4	3,4,5	
6388	G3	0.32	16.83	1	Illingworth and Freeman 1974
6397	F5	0.13	12.30	1	Cannon 1974
6401	(F+)	0.79	16.6:	6	
6402 (M14)	F8	0.58	16.90	1	Kogon <i>et al.</i> 1974
Pal 6	(F-)	1.80 ^a	18.0:	3	
6426	F8	0.40	17.3	4,5	
6440	G5	1.01	16.4:	5,6	
6441	G4	0.45	16.50	1	Hesser and Hartwick 1976a
6496	(G)	0.07	14.3:	5,6	
6517	F8	1.14	18.1:	2	Harris 1975
6522	F8	0.50	15.64	1	Arp 1965b
6528	(G)	0.63	16.4	1	van den Bergh 1971
6535	(F-)	0.36	16.1	3,4	
6539	(G)	1.22	15.7:	5	
6541	F6	0.13	14.60	1	Alcaino 1971a

TABLE II (*continued*)

NGC	Sp.T.	E_{B-V}	$(m - M)_V$	Method	Source
6544	F9	0.63	15.2:	5,6	
6553	G4	0.79	16.35	1	Hartwick 1975
6558	(F+)	0.40	16.1	4	
IC1276	(G)	0.92	18.5	3,4	
6569	G4	0.63	16.5	4,5,6	
6584	F7	0.11	16.4:	5,6	
6624	G4	0.25	15.20	1	Liller and Liller 1975
6626 (M28)	F8	0.33	14.9	3,4,6	
6637 (M69)	G5	0.17	15.65	1	Hartwick and Sandage 1968
6638	G2	0.36	16.8	3,5,6	
6642	(F+)	0.36	14.8	4,6	
6652	G2	0.11	17.0:	5,6	
6656 (M22)	F5	0.35	13.55	1	Arp and Melbourne 1959
Pal 8	(G)	0.30	18.4	3	
6681 (M70)	G0-G1	0.07 ^b	15.40	1	Harris 1975
6712	G4	0.35	15.51	1	Sandage and Smith 1966
6715 (M54)	F7	0.14	17.11	1	Harris 1975
6717	(G)	0.18	16.5	3	
6723	G2	0.01	14.80	1	Menzies 1974a
6752	F6	0.01	13.20	1	Cannon and Stobie 1973
6760	F8	0.91	15.9	3,4,6	
6779 (M56)	F5	0.22	15.60	1	Barbon 1965
Pal 10	(F-)	1.20 ^a	18.6	3	
6809 (M55)	F5	0.07	14.00	1	Harris 1975
Pal 11	(F-)	0.15 ^a	17.6	3	
6838 (M71)	G5	0.28	13.90	1	Arp and Hartwick 1971
6864 (M75)	F8	0.17	16.85	1	Harris 1975
6934	F7	0.12	16.22	1	Harris and Racine 1973
6981 (M72)	G0-G1	0.03	16.29	1	Dickens 1972a
7006	F3-F4	0.13	18.12	1	Sandage and Wildey 1967
7078 (M15)	F3	0.07	15.26	1	Sandage 1970
7089 (M2)	F3	0.06	15.45	1	Harris 1975
7099 (M30)	F3	0.01	14.60	1	Dickens 1972b
Pal 12	(F-)	0.02 ^a	19.0:	3,4	
Pal 13	(F-)	0.05	17.10	1	Ciatti <i>et al.</i> 1965
7492	(F-)	0.00	16.70	1	Barnes 1968

Key to methods of distance determination:

- (1) V_{HB} from CM diagram (reference in last column).
- (2) Giant branch of CM diagram fitted to standard cluster.
- (3) 25 brightest stars (Sawyer Hogg 1959; Arp 1965a).
- (4) $\langle m_{pg} \rangle_{RR}$ for cluster variables (Sawyer Hogg 1973).

(5) Richness index IR correlated with M_{V_f} (Kukarkin 1974).

(6) Visual degree of resolution of cluster (van den Bergh 1967b).

^a Reddening from cosecant law (see Sec. II of the text).^b Reddening from individual CM study (see last column for source).

clusters the moduli are not likely to be known *more* accurately than $\pm 0.^m05$. Combining $\pm 0.^m2$ with the adopted error margin of $\pm 0.^m3$ for $M_V(HB)$ itself then implies that the distance moduli as listed in Table II should have true *external* errors of $\pm 0.^m35$.

For the remaining 37 clusters in Table II, the distance moduli were calculated through the four secondary methods. All of these techniques were calibrated directly through the clusters in the primary list of 74, so that the $(m - M)_V$ estimates for the entire set are placed on a homogeneous system with a uniform distance scale. Of the 37 clusters in the secondary group, moduli for 22 could be obtained through the 25-brightest-stars method, 17 through $\langle m_{pg} \rangle_{RR}$, 18 through the richness index correlated with M_{V_f} , and 21 through the degree-of-resolution method. Thus, for most of them, more than one method was available; the individual results were averaged with half-weight given to the latter two techniques. Encouragingly, the four secondary approaches agreed well (to $< 0.^m5$) in most of the cases of overlap.

As discussed earlier, the $(m - M)_V$ values from the secondary methods are expected to have *random* errors near $\pm 0.^m5$, as compared with $\pm 0.^m2$ or less from the primary CM diagram method. However, every effort has been made to ensure that all the $(m - M)_V$ results are *systematically* accurate and homogeneous. The major difference between the present compilation and ones by previous writers (e.g., Kinman 1958; Arp 1965a; Kukarkin 1974; Peterson and King 1975; Woltjer 1975) is one of precision: Most of the clusters can now be put into the primary category of distances based on CM diagrams alone, with a resultant substantial improvement in reliability.

The data in Table II are presented as follows:

Column 1: cluster identification.*Column 2:* integrated spectral type of the cluster, used as an indicator of heavy-element abundance. These are taken from Kinman (1959a), or from Kron and Mayall (1960) for clusters not in Kinman's list. Burstein and McDonald (1975) have transformed the Kron-Mayall

spectral types onto Kinman's system, and their results are used here. For the clusters with no published spectral types, an attempt has been made to classify each one roughly into one of three categories: F- (low metallicity, in the range F2-F5), F+ (intermediate metallicity, F6-F9), or G (high metallicity, G0-G5). This has been done on the basis of their CM diagram morphologies (where available) and from their intrinsic integrated colors ($B - V$)₀ combined with the well-known relation between color and spectral type (Racine 1973; Burstein and McDonald 1975). The distant Palomar clusters, most of them evidently sparse and metal-poor, have been classified more or less arbitrarily as F- by analogy with the few whose metallicities have been directly measured.

Column 3: adopted foreground reddening. The E_{B-V} values are taken from the most recent compilation by Racine (1976) or from the individual CM studies in a few cases. In most cases the reddenings in Racine's list are similar to those in the earlier compilations (Racine 1973; Harris and van den Bergh 1974; Burstein and McDonald 1975). Those clusters which do differ significantly are ones whose integrated colors have recently been remeasured by Racine, so that the new E_{B-V} values are preferred. Finally, for the nine remaining clusters with no other available reddening estimates, a cosecant law of the form $E_{B-V} = 0.06 (\csc |b| - 1)$ has been used. This was derived from a plot of the E_{B-V} values from Racine's list versus cluster latitude $|b|$, along with the assumption that $E_{B-V} \approx 0.0$ at the poles (e.g., Philip and Tifft 1971; McClure and Crawford 1971; Sandage 1972, 1973; Philip 1974). In the table, the reddenings taken from Racine's list are unmarked, while those determined from the individual CM studies or the cosecant law are specially marked.

Column 4: distance modulus. Values of $(m - M)_V$ marked by colons are those derived only from the weakest secondary methods (cf. Sec. I), and which may therefore still be uncertain by more than $\pm 0.^m 5$.

Column 5: methods used to determine $(m - M)_V$. The key to these is given at the end of the table.

Column 6: reference sources used for the clusters with CM diagrams.

The combined data in Table II now provide up-to-date distance moduli and reddenings on a homogeneous system for 111 globular clusters.

It may be noticed from Table II that several clusters still remain with uncertain ($\gtrsim \pm 0.^m 5$) distance moduli, and that substantial work in this direction is still needed despite the enormous observational gains during the last few years. Most of the remaining clusters without high-quality distance estimates are, of course, in the galactic center region. These objects are generally highly reddened and in crowded star fields, so that obtaining reliable CM diagrams to the horizontal branch and below is frequently quite difficult. However, the foregoing discussion strongly indicates that the most promising secondary method of distance estimation is the

brightest-stars technique or some variant of it. It is suggested here that this approach can provide accurate distance moduli (with expected errors of $\lesssim 0.^m 3$) when cluster metallicity and population are properly considered. For the "problem" clusters in the galactic center group, such a technique may in fact be the best one since reliable photometry can often be obtained only for the brightest cluster stars in any case.

III. LOCATION OF THE CLUSTERS IN SPACE

The next step in the discussion is to calculate the space coordinates of the clusters. The intrinsic distance moduli of the clusters in Table II were obtained from $(m - M)_0 = (m - M)_V - 3.3 E_{B-V}$. The adopted ratio of total to selective absorption is $R = A_V/E_{B-V} = 3.3 \pm 0.3$ (Aannestad and Purcell 1974; Herbst 1975), although as will be seen later, its precise value is not critical for this discussion. From $(m - M)_0$ the distance D_\odot of each cluster from the Sun is obtained, along with the conventional distance components X, Y, Z defined in a coordinate system centered on the Sun,

$$\begin{aligned} X &= D_\odot \cos b \cos l, \\ Y &= D_\odot \cos b \sin l, \\ Z &= D_\odot \sin b. \end{aligned} \quad (11)$$

The coordinates X, Y, Z , and D_\odot are listed in Table III for all 111 clusters on our working list. In the last column of this table, r denotes the distance of each cluster from the galactic center, which is determined once R_0 is known (Sec. IV).

The positions of the clusters in space are plotted in Figs. 1-3, for the XZ , XY , and YZ coordinate planes. It is immediately evident from Figs. 1 and 2 that severe selection effects still exist in the present sample. As one moves along the X axis toward the galactic center, beyond $X \approx 9$ kpc the number of clusters seen near the galactic plane ($|Z| < 2$ kpc) drops sharply. This demonstrates clearly that our observed sample of clusters is seriously incomplete in this region: Many more clusters lying near the direction of the galactic center must still await measurement or discovery.

The true symmetry of the globular cluster system is best visible in the YZ plane of Fig. 3, which is least affected by the biases along the X axis. Here, the clusters lie in an essentially spherical halo, strongly concentrated toward the origin but also spreading well past the boundaries of the diagram at 20 kpc. The importance of using the YZ plane to study the space distribution of the clusters will be seen in detail in subsequent sections.

IV. THE DISTANCE TO THE GALACTIC CENTER

The distance information of Table III may next be applied to determine the true centroid of the cluster system and hence R_0 . A firm lower limit to R_0 can

TABLE III. Galactic distance components for globular clusters.^a

NGC	D_\odot	X	Y	Z	r	NGC	D_\odot	X	Y	Z	r
104	4.6	1.9	-2.7	-3.3	7.8	6355	6.6	6.6	-0.1	0.6	2.0
288	8.7	-0.1	0.1	-8.7	12.2	6356	18.9	18.4	2.2	3.3	10.7
362	8.9	3.2	-5.2	-6.4	9.8	6362	7.1	5.6	-3.8	-2.1	5.3
1261	13.4	0.1	-8.2	-10.6	15.8	6366	4.5	4.1	1.4	1.2	4.8
Pal 1	45.8	-27.8	33.2	15.0	51.4	6388	14.3	13.7	-3.5	-1.7	6.5
1851	10.8	-3.8	-8.0	-6.2	15.9	6397	2.4	2.2	-0.9	-0.5	6.4
1904	13.5	-8.0	-8.6	-6.6	19.8	6401	6.3	6.3	0.4	0.4	2.3
2298	12.2	-4.9	-10.7	-3.4	17.5	6402	9.9	9.0	3.5	2.5	4.3
2419	92.9	-84.0	-0.6	39.7	100.7	Pal 6	2.6	2.6	0.1	0.1	5.9
2808	9.2	1.9	-8.9	-1.8	11.2	6426	15.7	13.3	7.1	4.4	9.6
Pal 3	95.5	-35.3	-61.7	63.8	99.0	6440	4.1	4.1	0.6	0.3	4.5
3201	4.4	0.6	-4.3	0.7	9.1	6441	10.1	10.0	-1.1	-0.9	2.1
Pal 4	93.3	-27.0	-11.1	88.7	96.1	6496	6.5	6.3	-1.3	-1.1	2.8
4147	17.5	-1.2	-3.7	17.1	19.9	6517	7.4	6.9	2.4	0.9	3.0
4372	4.8	2.5	-4.1	-0.8	7.3	6522	6.3	6.3	0.1	-0.4	2.3
4590	9.6	3.8	-6.7	5.7	10.0	6528	7.3	7.3	0.1	-0.5	1.3
4833	5.4	2.9	-4.4	-0.8	7.1	6535	9.6	8.4	4.3	1.7	4.7
5024	17.2	2.7	-1.4	16.9	17.9	6539	2.2	2.0	0.8	0.3	6.5
5053	15.1	2.7	-1.2	14.9	16.0	6541	6.8	6.6	-1.2	-1.3	2.6
5139	5.2	3.1	-3.9	1.3	6.7	6544	4.2	4.2	0.4	-0.2	4.3
5272	10.0	1.5	1.3	9.8	12.2	6553	5.6	5.6	0.5	-0.3	3.0
5286	8.8	5.7	-6.5	1.6	7.2	6558	9.0	9.0	0.0	-0.9	1.1
5466	14.4	3.0	2.7	13.8	15.1	IC1276	12.4	11.4	4.6	1.2	5.6
5634	21.6	13.4	-4.3	16.4	17.6	6569	7.7	7.6	0.1	-0.9	1.3
5694	29.3	22.4	-12.1	14.6	23.5	6584	16.1	14.7	-4.8	-4.6	9.1
IC4499	18.4	10.5	-13.7	-6.5	15.3	6624	7.5	7.4	0.4	-1.0	1.5
5824	23.5	19.4	-10.0	8.9	17.2	6626	5.8	5.7	0.8	-0.6	3.0
Pal 5	26.7	18.6	0.3	19.2	21.7	6637	10.4	10.3	0.3	-1.9	2.6
5897	12.0	9.9	-3.0	6.1	6.9	6638	13.3	13.0	1.8	-1.7	5.2
5904	7.2	4.9	0.3	5.2	6.4	6642	5.3	5.2	0.9	-0.6	3.5
5927	7.2	6.0	-4.0	0.6	4.7	6652	21.3	20.8	0.6	-4.2	13.0
5946	9.3	7.9	-5.0	0.7	5.1	6656	3.0	2.9	0.5	-0.4	5.6
5986	10.0	9.0	-3.8	2.3	4.5	Pal 8	30.3	29.2	7.3	-3.6	22.3
6093	8.3	7.7	-1.0	2.8	3.0	6681	10.8	10.5	0.5	-2.3	3.2
6101	12.2	8.7	-7.9	-3.3	8.6	6712	7.4	6.7	3.2	-0.6	3.7
6121	2.4	2.3	-0.4	0.7	6.3	6715	21.4	20.6	2.0	-5.2	13.3
6139	8.9	8.5	-2.7	1.1	2.9	6717	15.2	14.5	3.3	-2.9	7.5
6144	7.6	7.3	-1.0	2.1	2.6	6723	9.0	8.6	0.0	-2.7	2.7
6171	5.8	5.3	0.3	2.3	3.9	6752	4.3	3.6	-1.6	-1.9	5.5
6205	7.2	2.8	4.7	4.7	8.7	6760	3.8	3.1	2.2	-0.3	5.6
6218	5.4	4.7	1.3	2.4	4.7	6779	9.4	4.3	8.3	1.4	9.4
6229	27.1	5.8	19.9	17.6	26.6	Pal 10	8.5	5.2	6.7	0.4	7.5
6235	11.7	11.4	-0.2	2.7	4.0	6809	5.7	5.2	0.8	-2.2	4.1
6254	4.4	3.9	1.0	1.7	5.1	Pal 11	26.4	21.6	13.4	-7.1	20.0
6266	5.9	5.8	-0.7	0.8	2.8	6838	3.9	2.2	3.3	-0.3	7.2
6273	10.5	10.3	-0.6	1.7	2.5	6864	18.1	15.3	5.7	-7.9	11.8
6284	10.5	10.4	-0.3	1.8	2.6	6934	14.6	8.5	10.9	-4.7	11.9
6287	8.4	8.2	0.0	1.6	1.6	6981	17.3	11.9	8.4	-9.4	13.0
6293	7.5	7.4	-0.3	1.0	1.5	7006	34.5	14.4	29.2	-11.5	31.9
6304	5.2	5.2	-0.4	0.5	3.4	7078	10.1	3.8	8.2	-4.7	10.5
6316	10.6	10.5	-0.5	1.1	2.3	7089	11.2	5.4	7.3	-6.6	10.3
6325	6.5	6.4	0.1	0.9	2.3	7099	8.2	5.0	2.6	-6.0	7.4
6333	8.0	7.8	0.8	1.5	1.8	Pal 12	61.2	35.5	20.9	-45.3	56.7
6341	7.8	2.4	6.0	4.5	9.7	Pal 13	24.4	0.9	17.9	-16.5	25.5
6342	15.0	14.8	1.3	2.5	6.9	7492	21.9	5.8	7.8	-19.6	21.3
6352	5.4	5.0	-1.7	-0.7	3.9						

^a All distances are in kiloparsecs. The values of r have been calculated assuming $R_0 = 8.5$ kpc.

quickly be obtained simply by averaging the X coordinates of all the clusters listed, without correcting for the obvious biases in the sample against distant low-latitude clusters. For the 106 objects in Table III within 40 kpc of the center, the centroid is

$$\langle X \rangle = 7.28 \pm 0.57 \text{ kpc (s.e.)}$$

$$\langle Y \rangle = 0.40 \pm 0.58 \text{ kpc (s.e.)}$$

$$\langle Z \rangle = 0.26 \pm 0.61 \text{ kpc (s.e.)}$$

As expected, $\langle Y \rangle$ and $\langle Z \rangle$ are both essentially zero; and the value for $\langle X \rangle$ already establishes that $R_0 \gtrsim 7$ kpc.

The selection effects in the sample of clusters along the X axis can be circumvented in a number of ways to determine the true centroid. Fernie (1962) chose to use a simple, more or less arbitrary functional form for the number density of clusters along the X axis, $N(X)$, along with the assumption that the actual value for $N(X)$ is known in the solar neighborhood. Arp (1965a) chose instead to calculate the centroid $\langle X \rangle$ for all clusters that

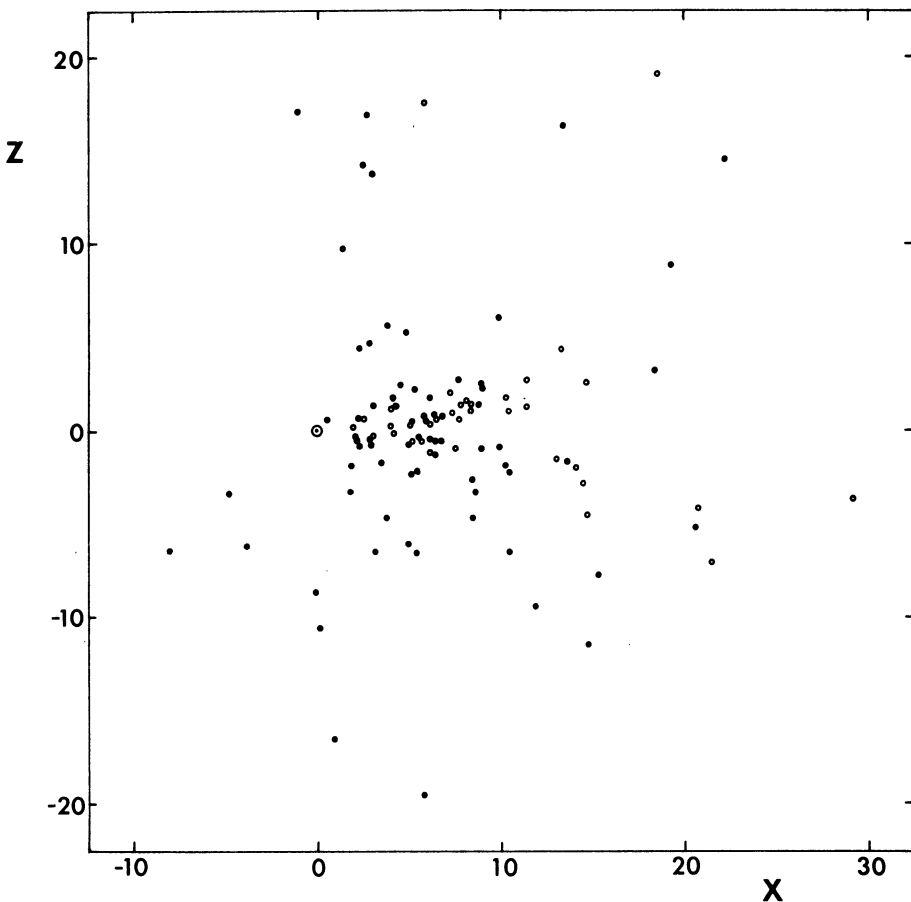


FIG. 1. Locations in space of the globular clusters, projected on the XZ coordinate plane. The position of the Sun is shown by a circled dot. Closed circles represent the clusters in the primary distance list (those with distance moduli from CM diagrams) and open circles represent clusters in the secondary list (those with distance moduli from the lower-quality methods).

lay well above the plane (specifically, those with $Z > 2.5$ kpc), thus avoiding the problematic low-latitude clusters entirely. Unfortunately, the data sample available to him was far less complete than the present one, so that eventually his result for R_0 was based on only 17 clusters.

The method adopted here is a simple generalization of Arp's. It is clear from inspection of the XZ plane (Fig. 1) that, the farther one looks away from the galactic plane, the less biased toward the Sun is the observed space distribution of the clusters. We may then consider only those clusters with coordinates $|Z|$ larger than some height above the plane Z_{lim} , and calculate the mean $\langle X \rangle$ for this restricted sample. This can be done for several different values of the cutoff height Z_{lim} . Ideally, as Z_{lim} increases from zero, the mean $\langle X \rangle$ should also increase until it approaches asymptotically its "true" centroid value of R_0 . The actual answer for R_0 should then be determined by the observed curve of $\langle X \rangle$ vs Z_{lim} . The advantages of this approach are that *all* the available cluster data are used, yet no particular form for the cluster space distribution is assumed.

The results, for the sample of 106 clusters within 40 kpc of the center, are presented in Table IV and plotted

in Fig. 4. In the table, column 1 gives Z_{lim} , column 2 the number of clusters with $|Z| > Z_{\text{lim}}$, column 3 the mean $\langle X \rangle$ coordinate for these N objects, and column 4 the internal standard error for the value of $\langle X \rangle$. The mean X does indeed increase rapidly for small values of Z_{lim} , then stabilizes at a roughly defined upper envelope of about 8.5 kpc. In practice, to decide on a value for R_0 a compromise must be made between the two competing effects of systematic and random error: As Z_{lim} increases, $\langle X \rangle$ approaches R_0 and hence becomes a more *accurate* estimator of the centroid. Yet at the same time, the value of $\langle X \rangle$ becomes less *precise* as the number of available clusters N decreases and the internal error $\sigma(\langle X \rangle)$ goes up. As seen in Fig. 4, the rapid increase in $\langle X \rangle$ for small values of Z_{lim} is large enough compared with the internal errors to be significant. Beyond $Z_{\text{lim}} \approx 3$ kpc, the internal error σ becomes so large ($\gtrsim 1.5$ kpc) that no noticeable systematic changes occur any longer in the value of $\langle X \rangle$ and the method becomes insensitive. (The apparent minimum in $\langle X \rangle$ beyond $Z_{\text{lim}} \approx 3$ kpc, though it may possibly be due to a small incompleteness in the sample of extremely distant high-latitude clusters, is therefore not significant.) Consequently, we adopt an intermediate value for Z_{lim} and use the corresponding

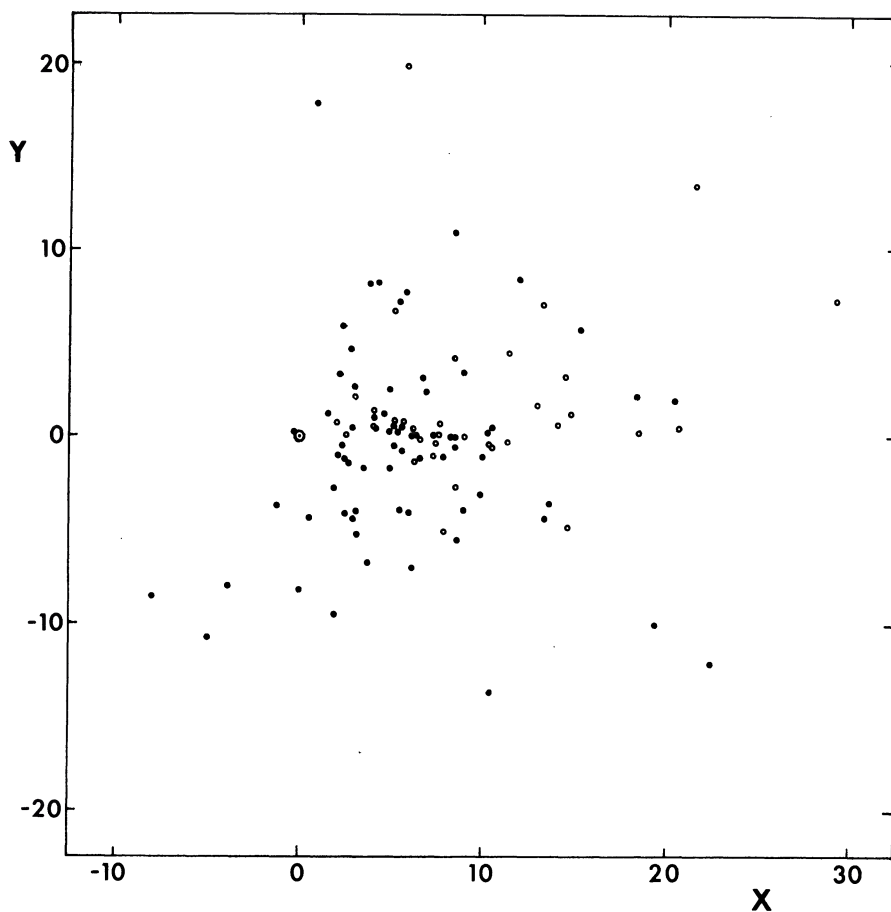


FIG. 2. Locations of the globular clusters as projected on the plane of the disk, in the XY coordinate frame. Symbols are as defined in Fig. 1.

$\langle X \rangle$ value to fix R_0 . From Fig. 4, we adopt a best estimate of $R_0 = 8.5$ kpc, where the curve appears most nearly to level off. At this point ($Z_{\text{lim}} \simeq 2.5$ kpc) the internal standard error in $\langle X \rangle$ is ± 1.2 kpc.

It remains to discuss the effects of the underlying assumptions upon this measurement of R_0 . The most critical of these is the cluster distance scale itself [i.e., the assumed $M_V(\text{HB})$]. To test the effects of altering the cluster distances, the calculation in Table IV was redone with a uniform change in $M_V(\text{HB})$ by $\pm 0.^m 3$. The result for R_0 changed correspondingly by ± 1.0 kpc (see Fig. 4). This implied uncertainty in R_0 is therefore comparable to the internal random error of the method itself.

Next, suppose that the more metal-rich clusters in the sample (those with G-type spectra) actually have fainter horizontal branches near $M_V(\text{HB}) \simeq 1.0$, as would be indicated from the main-sequence photometry of 47 Tucanae (Hartwick and Hesser 1974) or Christy's theoretical picture. This turns out to have virtually no effect ($\lesssim 0.2$ kpc) on the estimate of R_0 , because the G-type clusters are almost all located at low Z values near the plane and they are the first to be eliminated as Z_{lim} increases. Our method of obtaining R_0 thus depends

mostly on the metal-poor (F-type) clusters, for which the uniform assumption $M_V(\text{HB}) = 0.6$ should be more reliable. It is also important to emphasize that this method depends principally on just those clusters for which the distances are most accurately determined. Of the 46 clusters with $|Z| > 2.5$ kpc in the sample, distance moduli for 37 were taken directly from CM diagrams and are therefore accurate to $\lesssim 0.^m 3$. This, combined with their low foreground reddenings ($\langle E_{B-V} \rangle = 0.1$), minimizes the possibility of any systematic error in the value for R_0 that may result from the individual cluster distances alone.

For similar reasons, realistic changes in the adopted cluster reddenings or in $R = A_V/E_{B-V}$ have negligible effects on R_0 . The clusters with $|Z| > 2.5$ kpc have low reddenings to begin with, so changes in R (e.g., by ± 0.5 from our assumed value of 3.3) or in the E_{B-V} estimates in Table II by ± 0.05 do not affect the result for R_0 by more than 0.3 kpc in either direction.

Finally, the effect of sample incompleteness may be discussed. It has already been mentioned that there are likely to be many more low-latitude clusters beyond the galactic center which are not included in our sample. But because our determination of R_0 depends mostly on the

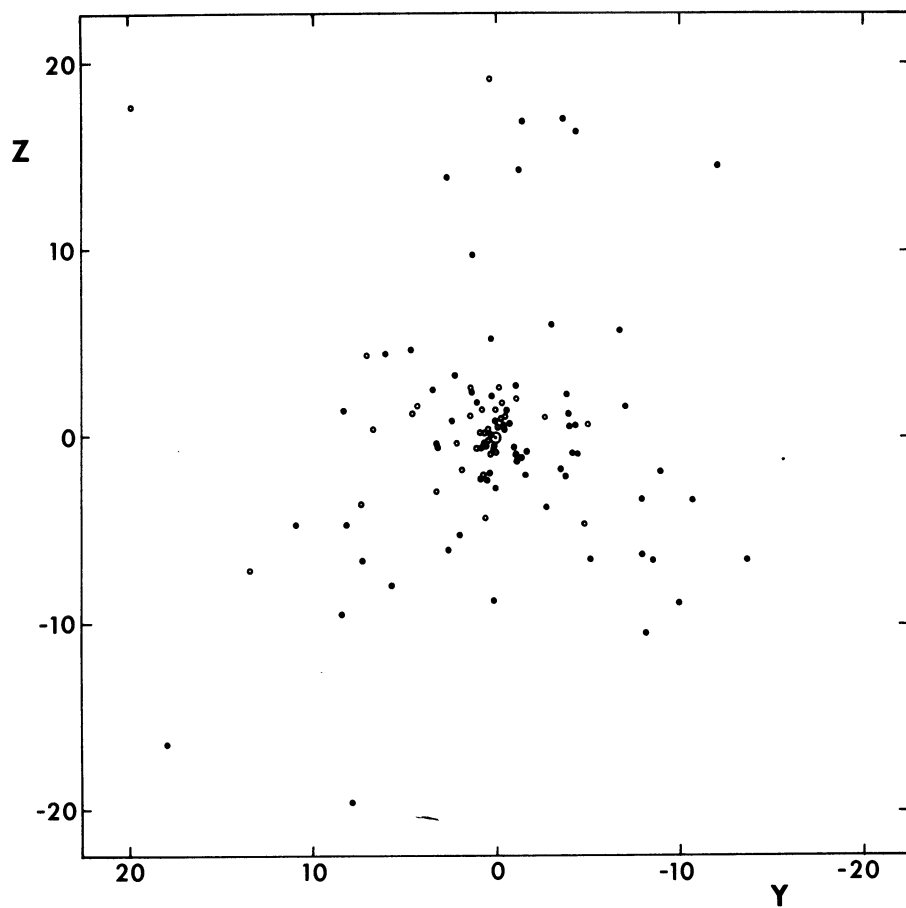


FIG. 3. Locations of the globular clusters in the YZ coordinate plane. Symbols are as defined in Fig. 1. This diagram best shows the true spherical symmetry of the cluster distribution.

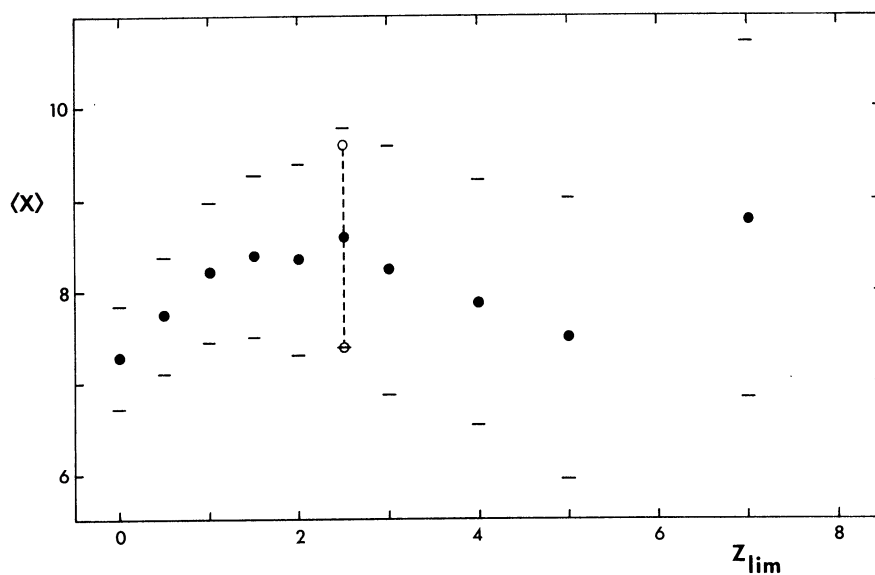


FIG. 4. Determination of the distance to the galactic center. Here $\langle X \rangle$ denotes the mean X coordinate for all clusters farther from the plane than Z_{lim} , as in Table IV. The tick marks above and below each point represent the internal standard error $\sigma(\langle X \rangle)$. The two open circles attached by the dotted line through the point for $Z_{\text{lim}} = 2.5$ kpc show the effect of changing the entire cluster distance scale $M_V(\text{HB})$ by 0^m3 in either direction.

TABLE IV. Calculation of R_0 .

Z_{lim}	N	$\langle X \rangle$	$\sigma(\langle X \rangle)$
0.0 kpc	106	7.28 kpc	0.57 kpc
0.5	93	7.75	0.64
1.0	75	8.22	0.77
1.5	65	8.40	0.88
2.0	53	8.36	1.04
2.5	46	8.59	1.20
3.0	40	8.23	1.36
4.0	35	7.88	1.33
5.0	28	7.49	1.54
7.0	18	8.78	1.94

high-latitude clusters, this serious incompleteness at low latitudes does not affect the result for R_0 at all. By contrast, the sample of high-latitude clusters is far more complete (see the discussion by Arp 1965a on this point). The Palomar Sky Survey and extensions, covering 80% of the sky, have been thoroughly searched for high-latitude clusters and it would appear that very few such objects (at least within $r \sim 40$ kpc) can be added to the ~ 50 known with $|Z| > 2.5$ kpc. It is therefore concluded tentatively that any existing incompleteness in the cluster sample at high latitudes is small and will not have a serious effect on R_0 .

In summary, the only factors on which this measurement of R_0 depends significantly appear to be (a) overall changes in the distance scale $M_V(\text{HB})$; and (b) any serious incompleteness in the observed sample of clusters farther than 2 kpc from the plane and within $r \sim 40$ kpc.

We adopt $R_0 = (8.5 \pm 1.6)$ kpc for the following discussion, where the quoted error (s.e.) is the combination of the internal random error of ± 1.2 kpc (Table IV) and the external error of ± 1.0 kpc from the uncertainty in $M_V(\text{HB})$. This result agrees closely with other recent determinations of R_0 that have been made from the RR Lyrae and main-sequence stars in the galactic center region (Oort and Plaut 1975; van den Bergh 1974) or from the kinematics of stars in the galactic disk (Toomre 1972; Thackeray 1972; Rybicki *et al.* 1974; Balona and Feast 1974; Crampton and Georgelin 1975). Table V summarizes the estimates obtained from five of these methods (not all of them, of course, are completely independent). An average of these weighted inversely as the quoted errors yields an overall result of $R_0 = (8.8 \pm 0.7)$ kpc. (The actual weighting scheme adopted has only negligible effects on the resulting average, since the five individual R_0 values agree closely to begin with.) Although it does not seem possible yet to eliminate the older "standard" value of 10 kpc with certainty, all the most recent determinations definitely favor a somewhat smaller number.

V. THE NUMBER OF GLOBULAR CLUSTERS IN THE GALAXY

Once R_0 is known, many fundamental properties of the globular cluster system can be found. Perhaps the

simplest of these is the total number of globular clusters in the Galaxy, a quantity which may readily be estimated from the present data.

In Table III, 77 clusters out of the total of 111 lie on the Sun's side of the galactic center (i.e., 77 ± 10 have $X < R_0$, where the quoted error corresponds to ± 1.6 -kpc uncertainty in R_0 itself). In addition to the objects in Table III, there are also 18 more *known* clusters with no distance estimates (Alter *et al.* 1970; Kukarkin 1974) and it is reasonable to assume that at least half of these also lie on the Sun's side of the center (since most of these 18 are near the galactic center). Thus, there are approximately 85 ± 15 known clusters with $X < R_0$. There should, of course, be equally many on the far side of the galactic center, so that by symmetry arguments alone we must conclude that there are ~ 170 globular clusters in the Galaxy. Only 129 of these are listed in present catalogs (cf. Alter *et al.* 1970 or Kukarkin 1974), so that 40 or more new clusters must still await discovery. Of course, most of these will lie in the highly obscured galactic center region and at distances $X > 8$ kpc.

The estimate of 170 clusters is, furthermore, only a lower limit to the true total number since it does not allow for any incompleteness in our knowledge of the low-latitude clusters on the Sun's side of the galactic center. Adding in a 10%–20% incompleteness fraction for $X < R_0$ would raise the total number to $\sim 190 \pm 30$ globular clusters in the whole Galaxy. Racine (1975, unpublished) in recent work along similar lines, specifically estimated the number of undiscovered clusters as a function of latitude and angular distance from the galactic center, and concluded similarly that the total population should be near 200 or even more. Certainly the statement by Arp (1965a) that the total is as low as 126 ± 7 now appears to be a serious underestimate.

VI. METALLICITY PROPERTIES OF THE SPACE DISTRIBUTION

A. Distribution of Metallicity Groups

One of the most outstanding and significant properties of the galactic globular cluster system is the correlation between a cluster's heavy-element abundance and its galactocentric position. This feature has been well established for many years (Mayall 1946; Morgan 1956,

TABLE V. Recent determinations of R_0 .

Reference	Method	Result (kpc)
Balona and Feast 1974	Distant OB stars	9.0 ± 1.6
Rybicki <i>et al.</i> 1974; Toomre 1972	Galactic disk model	9.0 ± 1.0
Oort and Plaut 1975	RR Lyrae stars in galactic nucleus	8.7 ± 0.6
van den Bergh 1974	Main-sequence stars in nucleus	9.2 ± 2.2
This paper	Globular cluster system	8.5 ± 1.6
	Mean	8.8 ± 0.7

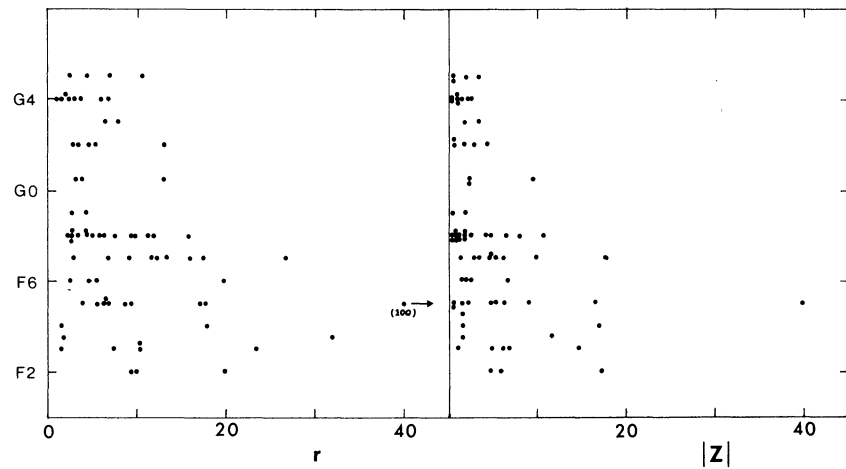


FIG. 5. Relation of cluster metallicity (integrated spectral type) to distance r from the galactic center or distance $|Z|$ from the galactic plane. The region close to the center ($r \lesssim 10$ kpc) is seen to be occupied by all types of clusters, whereas as r or $|Z|$ increase, the more metal-poor on the average the clusters become. The most distant point ($r \sim 100$ kpc) is for NGC 2419.

1959; Arp 1955, 1965a; Kinman 1959a), but with the greatly enlarged amount of information available here, certain of these characteristics can be demonstrated more explicitly than before.

Figure 5 shows the relation between cluster metallicity (as represented by the integrated spectral type, Table II) and its location in space, both in terms of the distance r from the center and the distance $|Z|$ away from the galactic plane. In each graph the trend is similar and well marked: Rough upper envelopes to the points may be drawn which specify the upper limit r_{\max} or $|Z|_{\max}$ at which a cluster of any given spectral type (metallicity) is seen. In this respect, r_{\max} and $|Z|_{\max}$ are equivalent metallicity parameters. We see that the most metal-poor clusters (F2–F5) may be found at any distance from the galactic center or plane, from $r \simeq Z \simeq 0$ out to the limits of the halo. But as the spectral type increases, the region of space in which the clusters can be found shrinks progressively, until the most metal-rich clusters (G0–G5) are almost completely restricted to positions well inside the Sun's orbit.

Although the clusters with highest heavy-element abundance can be found *only* near the galactic center, it is crucial to emphasize that the central region is not the exclusive domain of the most metal-rich objects. Instead, the farther in to the center one looks, the greater the range of cluster metallicities is seen. Clusters of low, intermediate, and high heavy-element abundance are all found with roughly equal frequency near the center. By contrast, in the outer halo regions the range of abundances seen in the clusters steadily becomes more and more restricted to the most metal-poor objects. The minimum metallicity found at *any* distance r is roughly spectral type F2, corresponding to a heavy-element content $Z \sim 10^{-4}$. This small but nonzero Z_{\min} value indicates that the protogalactic gas from which even the most metal-poor clusters condensed must already have been enriched by a small amount of heavy elements before the epoch of cluster formation, if the presently observed compositions of the cluster stars do represent their primordial abundances.

B. Ellipticity of the Cluster System

Another striking representation of the marked change in space distribution with metallicity type is shown in Fig. 6(a) and (b). Here, the locations of the clusters in the XZ and YZ projections are plotted as in Figs. 1 and 3, but with the objects now separated into the two categories of "metal-poor" (F-type spectra) and "metal-rich" (G-type spectra). The F-type clusters are again seen to occupy a far larger volume of space than their more metal-rich counterparts.

From some earlier discussions concerning the structure of the cluster system (Baade 1958; Kinman 1959a, 1959b; Arp 1965a) a conventional picture has been built up that the most metal-rich clusters lie in a moderately flattened space distribution towards the galactic plane. It may be noticed from Fig. 6(a) that both the G-type clusters and the inner F-type clusters appear to show a concentration toward the plane, as opposed to the clusters in the outer halo whose distribution is essentially spherical. Kinman (1959a) and Arp (1965a) concluded that the distribution of the G-type clusters could be described roughly by an ellipsoid with minor/major axial ratio $b/a \simeq 0.5$. On the other hand, Woltjer (1975) and Racine (1975, unpublished) concluded that $b/a \simeq 1$ even for the most metal-rich group by considering their distribution on the plane of the sky.

This apparent problem can be clarified by noting the cluster distributions carefully in each of the three planar projections (Figs. 1–3 and 6). If the G-type clusters are truly concentrated toward the disk, then their distribution should appear flattened in the XZ and YZ projections but *not* in the XY projection. Instead, in the actual diagrams the "flattening" appears for the central clusters in the XY and XZ planes but not the YZ plane. Thus, a large part of the apparent flattening [seen clearly, for example, in Fig. 6(a)] must be due simply to random errors in the estimated cluster distances, which tend to spread the clusters out along the line of sight and thus create an illusory ellipticity. And because the distances of the heavily reddened low-latitude clusters are the most

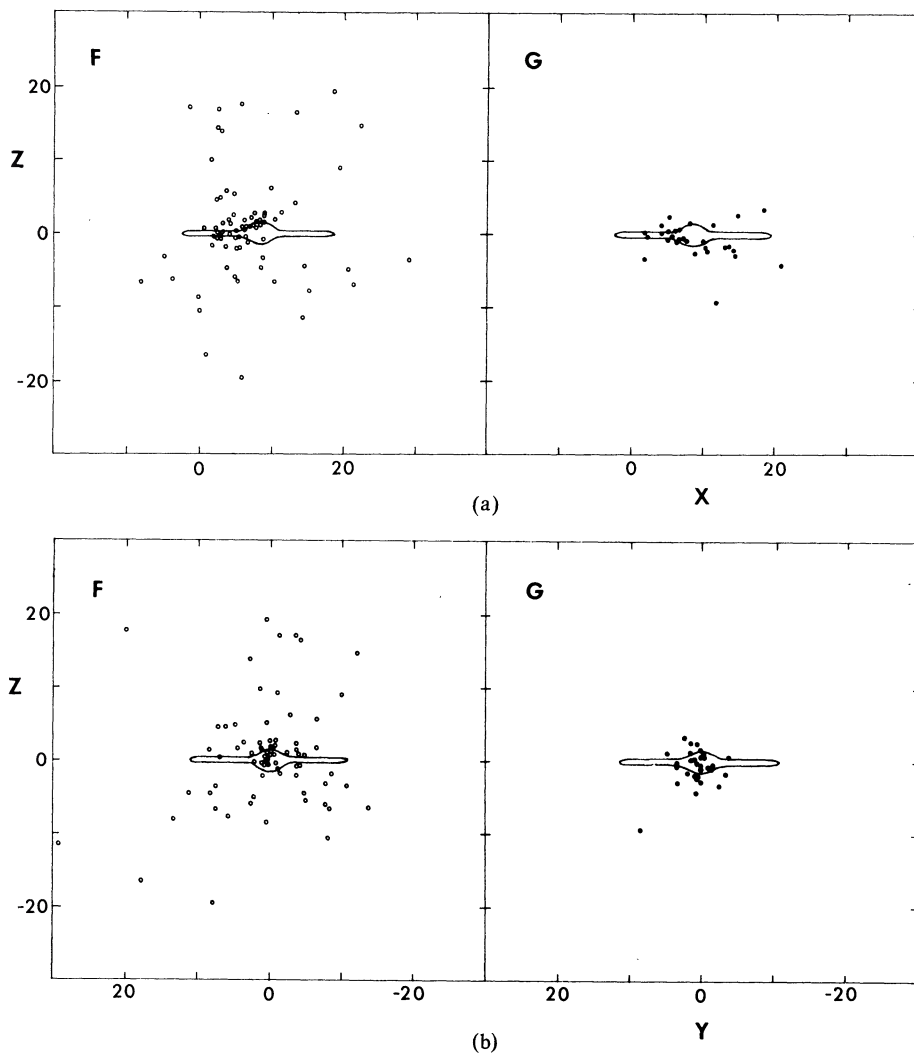


FIG. 6. (a) Space distributions of the F- and G-type clusters plotted separately, in the XZ coordinate plane. The F-type (metal-poor) clusters are plotted as open circles and the G-type (metal-rich) clusters as closed circles. (b) Space distributions of the F- and G-type clusters in the YZ plane.

uncertain, this effect will be largest for just those clusters near the galactic center. Furthermore, for *any* cluster located in a direction near the galactic center, almost the entire effect of any error in the distance estimate shows up along the X axis, since $X = D_{\odot} \cos b \cos l \simeq D_{\odot}$ for such clusters. By contrast its Y and Z coordinates are known far more precisely, being almost perpendicular to the line of sight; thus, the estimated distance to the cluster can be changed by a large amount and affect X severely yet leave the Y and Z components almost unchanged in absolute terms. Because the G-type clusters are all located near the galactic center, this means that purely random errors in their distances will produce a systematic error in the apparent ellipticity of their space distribution *in the XZ plane*. (Note that this distortion effect is much less important for the *outer* halo clusters, which are seen at high latitudes in almost all directions, and the effects of random distance errors are distributed more equally along the X , Y , and Z axes. Thus, their spherical distribution is preserved under purely random errors.)

The YZ plane, which is almost free of these distortion effects, is the most useful one for estimating the true ellipticity of the cluster system. This projection for the F- and G-type clusters is displayed in Fig. 6(b). No obvious flattening toward the disk is visible even for the most metal-rich group. This result emphasizes the serious effect of distance errors for the central clusters, and suggests that the true space distribution of all the metallicity types does not depart much from spherical symmetry. The conventional term "disk clusters" for the metal-rich group of globular clusters would therefore seem to be a misnomer; they should more properly be termed a "nuclear" or "inner halo" group associated with the central bulge of the galactic nucleus.

VII. THE OVERALL SPACE DISTRIBUTION

A. The Three-Dimensional Density Distribution

The aim of this section is to derive an explicit form for the density distribution in the cluster system, and to relate it to the galactic halo as a whole. Suppose first that

GLOBULAR CLUSTER SYSTEM

1109

TABLE VI. Density distribution of the cluster system by number and mass.

r range (kpc)	$N(r)$	$\log \varphi(r)$ (kpc^{-3})	$\log \rho(r)$ ($M_\odot \text{pc}^{-3}$)
1–2	6	-0.39	-4.34
2–3	11	-0.56	-4.41
3–4	7	-1.04	-4.99
4–5	7	-1.26	-5.28
5–6	7	-1.44	-5.39
6–7	5	-1.73	-5.09
7–8	7	-1.70	-5.43
8–9	1	-2.66	-6.15
9–10	5	-2.06	-6.03
10–12	4	-2.58	-5.93
12–14	2	-3.03	-6.76
14–16	4	-2.85	-6.66
16–18	2	-3.26	-6.97
18–20	2	-3.36	-7.30
20–30	3	-4.12	-8.33
30–60	0 (1) ^a	$-\infty$ (-5.60)	...
60–90	0 (3)	$-\infty$ (-5.55)	...
90–120	1 (2)	-6.32 (-5.84)	...
120–180	0 (3)	$-\infty$ (-6.46)	...

^a For the last four entries of $N(r)$, the first number is the total of “normal” globular clusters in the given r range, while the number in parentheses gives the total of “anomalous” outlying objects (see Sec. VII-C of the text).

the number density of globular clusters at distance r from the galactic center is given by some radial function $\varphi(r)$. The implicit assumption of spherical symmetry has been shown from the preceding discussion to be satisfactory or nearly so, for every metallicity group within the system.

The problem is now to determine $\varphi(r)$ from the observations. Its shape might be derived directly from all the data in Table III by adding up the number of clusters at each radius r , but this simple procedure would be incorrect and would lead to a significant bias with r . As described earlier, inspection of Figs. 2 or 6 shows that the available sample of clusters *near the galactic center* is far more complete on the Sun’s side of center. For example, in the region $0 < X < R_0$ there are 39 clusters within $|Z| < 2$ kpc, whereas in the analogous region on the far side ($R_0 < X < 2R_0$) only five appear. [Errors arising from this observed anisotropy are contained in some other earlier derivations of $\varphi(r)$; e.g., Arp (1965a), or Woltjer (1975).]

A simple way to counteract the anisotropy problem is to take only the clusters on the *near* side of the center ($X < R_0$) and then double them to form the total distribution. By symmetry our adopted space distribution for the far half is then just the mirror image of the near half. The incompleteness in the low-latitude clusters is therefore implicitly corrected for, and simultaneously those clusters ($X > R_0$) whose distances are most uncertain are removed in an unbiased way. We assume only that the sample is complete on the near side of the center, which is expected to be true or nearly so, except perhaps for the very innermost sphere ($r \lesssim 3$ kpc) nearest the center.

There are 73 clusters in the present sample (Table III)

with $X < R_0$ and $r \lesssim 40$ kpc. For this subset, which is taken to be the most nearly unbiased representation of the total system, the observed space distribution $\varphi(r)$ is as listed in Table VI and plotted in Fig. 7. In the table, $N(r)$ equals the total number of clusters out of the sample that fall in each given range of r ; $\varphi(r)$ then gives the number of clusters per unit volume in each shell. The final column gives $\rho(r)$, the *mass* density of globular clusters at each radius, obtained by adding up the masses of the individual clusters in each shell and dividing by the shell volume. The cluster masses were estimated in turn from their integrated absolute magnitudes M_{V_i} (e.g., Peterson and King 1975; Harris 1974) combined with an assumed mass-to-light ratio of 1.5 (Illingworth and Freeman 1974; Illingworth 1975) for all clusters.

The graph of $\varphi(r)$ in Fig. 7 immediately establishes that the radial distribution of the clusters falls off smoothly and steeply over the whole range of r . The points for the two innermost shells ($1 \leq r \leq 3$ kpc) are likely to be only lower limits because of the incompleteness problem near the galactic center already discussed. Beyond this, we are safer in assuming that the distribution plotted should represent the true distribution. The very outermost points ($r > 30$ kpc), where the objects become so sparsely spread that no easy or precise determination of $\varphi(r)$ is possible, present another special problem and are discussed separately below.

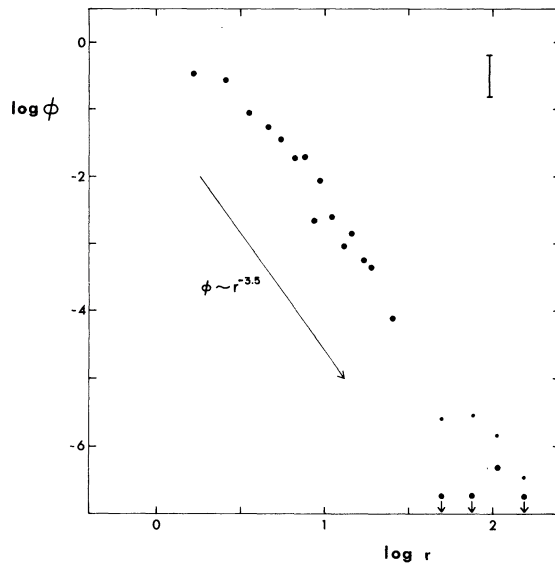


FIG. 7. The space density $\varphi(r)$ of the cluster system, as listed in Table VI. Here φ is the number of clusters/ kpc^3 , plotted as a function of r in kiloparsecs for each radial shell. The error bar at upper right shows the expected random error of the plotted points (approximately a factor of 2 in either direction). The φ curve is seen to follow closely a power law $\varphi \sim r^{-3.5}$ over most of its range. For the four outermost shells, the small dots denote the values of φ if all “anomalous” outlying systems (dwarf spheroidal systems and Palomar clusters) are included, whereas the large dots are the resulting values of φ for the four shells if only the “normal” objects (i.e., NGC 2419 alone) are included (see Sec. VII-C of the text).

Despite the difficulties mentioned, over most of the relevant range in r (3–30 kpc) the shape of $\varphi(r)$ can plainly be described by a single power law $\varphi \sim r^{-\alpha}$, where $\alpha = -\Delta \log \varphi / \Delta \log r \simeq 3.5$. A straightforward least-squares fit excluding the two uncertain innermost points gives $\alpha = 3.54 \pm 0.26$. Although the data points indicate superficially that the slope α may actually increase slightly outward (e.g., $\varphi \sim r^{-3}$ may be more appropriate for the inner points while for $r > 10$ kpc the distribution steepens to $\varphi \sim r^{-4}$), in view of the possible observational errors this trend may not be significant. The most reliable conclusion from Fig. 7 is that the density distribution of the globular cluster system lies almost certainly in the range $\varphi \sim r^{-3.5 \pm 0.5}$ and that this simple law applies over virtually the entire expanse of the halo.

For the distribution of *mass* in the cluster system, a plot of $\log \rho$ vs $\log r$ from Table VI quickly shows that the radial distribution of $\rho(r)$ parallels that of $\varphi(r)$, i.e., $\rho \sim r^{-3.5}$. [Somewhat more scatter is introduced in the $\rho(r)$ plot due to additional uncertainties in estimating the cluster masses and random fluctuations in the individual masses found in each shell.] The similarity of $\rho(r)$ and $\varphi(r)$ is expected, since the clusters at any given distance r tend to have the same masses as those closer in or farther out; that is, there is no noticeable trend in the available data for a change of average cluster mass with r . This may also be seen directly from a plot of the cluster luminosities M_{V_t} with r .

The value obtained here for the logarithmic slope α agrees well with corresponding density gradients determined for various types of Population II stars in the Galaxy, such as RR Lyrae variables or metal-poor giants (Oort 1965; Innanen 1973; Oort and Plaut 1975). Most of these results also give $\alpha \simeq 3\text{--}4$. Thus, the density gradient of the cluster system does seem to describe the distribution of normal Population II stars in the halo as a whole; i.e., they are “representative” halo objects in this respect. The unique power of using the clusters to measure $\varphi(r)$ is that they can be explicitly observed over the entire distance range needed to take in the complete halo of the Galaxy.

B. Relation of $\varphi(r)$ to Metallicity

Another question of interest is how $\varphi(r)$ will differ for different cluster metallicity groups, since it would conceivably provide a way of relating the times of formation of each metallicity grouping within the cluster system to the collapse phase of the protogalaxy. For instance, recent formation models for disk galaxies (Larson 1974, 1975, 1976) predict that the central concentration of the protogalaxy will increase rapidly during its collapse (assuming a start from a uniform-density cloud) until the infalling gas is turned mostly into stars, while at the same time the gas is being steadily enriched in heavy elements. Thus, the composition of a globular cluster would be expected to depend both on its distance from the center at time of formation and on the actual “mo-

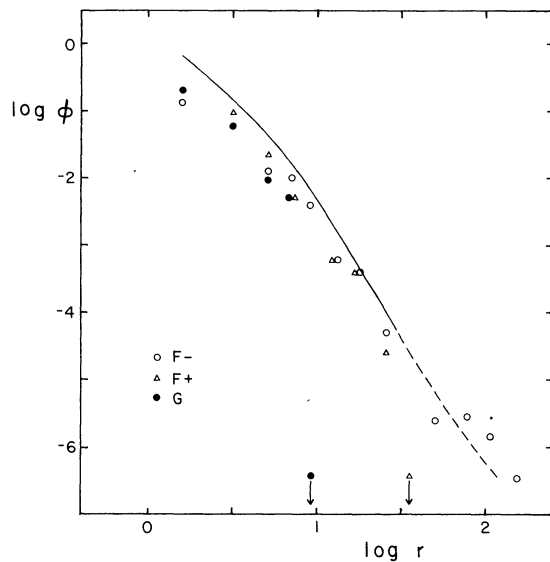


FIG. 8. The space density distributions $\varphi(r)$ for the three selected metallicity subgroups within the cluster system. The φ values for the most metal-poor clusters (F^-) are plotted as open circles; the intermediate clusters (F^+) as triangles; and the most metal-rich clusters (G) as closed circles. The smooth curve drawn in denotes the total $\varphi(r)$ curve for the cluster system as a whole, from Fig. 7 (the dotted extension of this curve past $\log r \simeq 1.5$ is very uncertain). Note particularly that beyond $\log r \simeq 0.9$, no G -type clusters are found (i.e., $\varphi_G \rightarrow 0$), and beyond $\log r \simeq 1.5$, no F^+ -type clusters are found ($\varphi_{F^+} \rightarrow 0$).

ment” during the collapse epoch at which it condensed from the infalling gas.

The relation of $\varphi(r)$ to metallicity is already partly seen in Fig. 5 (cluster spectral type versus r) but is shown more explicitly in Fig. 8. Here, the space density distribution $\varphi(r)$ is plotted separately for each of the three metallicity groups (F^- , F^+ , G) defined in Sec. II. We may denote the three component distributions as $\varphi_{F^-}(r)$, $\varphi_{F^+}(r)$, $\varphi_G(r)$. For $r \lesssim 7$ kpc (where all three metallicity groups are found), φ_{F^-} , φ_{F^+} , and φ_G decrease outward in quite similar fashion, parallel to the overall $\varphi(r)$ curve itself. Beyond ~ 7 kpc, no G -type clusters are found and φ_G drops rapidly to zero. Continuing outward, φ_{F^-} and φ_{F^+} remain parallel until $r \simeq 25$ kpc, beyond which no F^+ types are found and φ_{F^+} drops to zero in turn. Thus, where each type of cluster exists, we conclude from Fig. 8 that the three-component space distributions behave comparably with the total $\varphi(r)$ distribution. The principal differences among the three distributions appear to be where the outer boundaries are imposed on each—again, presumably because of the initial conditions of formation of the system as a whole.

The most important conclusion from Fig. 8 is simply that *all* types of globular clusters are strongly concentrated toward the galactic center. The approximate density law $\varphi \sim r^{-3.5}$ applies for every metallicity subgroup, at least out to the maximum radius for each subgroup. In particular, the density distribution for even

the most metal-poor group (which presumably formed earliest during the collapse phase) falls by at least five orders of magnitude from the center outward beyond $r \simeq 30$ kpc. It is, of course, true that if one considers the total shape of each of the three subdistributions, including the behavior of each one near its boundary r_{\max} where the density drops to zero, then the G-type clusters are most concentrated (i.e., have a larger overall value of α) to the center and the F- clusters the least. But it does not seem possible to isolate any subgroup which displays little or no central concentration at all.

Interpretation of these observed features of the cluster system relates strongly to the earliest history of the Galaxy and its "collapse" phase (Eggen, Lynden-Bell, and Sandage 1962; Sandage 1970; Hartwick and Hesser 1974). The observed strong density and metallicity gradients in the cluster system, as discussed here and in Sec. VI, correspond strikingly with the overall properties of the galactic halo predicted from the recently developed theory of Larson (1975, 1976) for the formation of spiral galaxies. Since this theory provides the first fully developed set of models for the formation of disk galaxies like our own, a brief comparison with the observations is appropriate here. In Larson's models the halo (spheroidal component) is formed in an early collapse phase lasting $\lesssim 10^9$ yr, whereby an initial rapid burst of star formation turns much of the infalling gas into stars. Both the strong density gradient and mean abundance gradient are "built into" the halo during the collapse, since the infalling gas density and subsequent star-formation and metal-enrichment rates increase rapidly toward the center. In the models, the remaining protogalactic gas left over after the initial violent burst gradually settles into a disk, with a much lower star-formation rate and consequent longer total formation period.

The model characteristics provide a natural framework for the rapid initial construction of (a) a strong density gradient throughout the halo, (b) a resultant small spread of formation times for the globular clusters of all metallicities, consistent with the available age measurements for observed clusters (Sandage 1970; Hartwick and Hesser 1974), and (c) a large range of heavy-element abundances built up in the central regions during the same brief initial burst. Other authors (Demarque and McClure 1976; Hesser, Hartwick, and McClure 1976) have already noted that this picture for the early development of a disk galaxy could also provide a means for understanding the detailed compositional differences observed between the extreme G-type globular clusters and the oldest open clusters. They conclude that the separate dynamical processes leading to the formation of the halo and disk may have led to different relative enrichments of the individual heavy elements in each type of cluster. The full details of the early creation process are clearly far from being completely understood; but the broad features of both the disk and halo as predicted from the recent models agree so persuasively with their observed characteristics that a new insight into the

physical processes during the formation period has almost certainly been achieved.

C. The Outermost Halo Systems

So far, the behavior of $\varphi(r)$ in the outermost part of the halo ($r \gtrsim 30$ kpc) has not been treated. In these distant regions the problem of determining φ becomes complicated not only by the extreme sparseness of the clusters but by the radically different and intriguing nature of the objects themselves. In the discussion of this section a brief attempt will be made to sort out from the available evidence (tantalizingly incomplete though it is at present) which objects can be said to "belong" to the cluster system in the outermost regions, and which ones may have formed or evolved in different ways.

The Population II objects more distant than $r \simeq 40$ kpc include several Palomar clusters (the ones in Table III are Pal 1, 3, 4, and 12), NGC 2419 (Racine and Harris 1975), and the six known dwarf spheroidal systems (Hodge 1971). [Although the dwarf spheroidal systems are not usually considered along with the globular clusters, as Population II objects of extremely low metallicity, advanced age, and globular-cluster-like total masses, they clearly belong in a discussion of the structure of the outer halo. In addition, possible connections between certain dwarf spheroidals and Palomar clusters have recently been pointed out (cf. the text following), even though the former objects are structurally somewhat different. Thus, it seems necessary to consider the status of each type of outer-halo object in the present discussion.] Observation of these objects remains extremely difficult simply because of their enormous distances. However, a summary of the available data suggests that with a single exception (NGC 2419), all the outlying systems that have so far been studied appear to share the following distinctive characteristics:

(1) All of them have diffuse, low-density structures that would not survive close tidal encounters with the Galaxy in their present form (e.g., Hodge 1971 and references cited; Burbidge and Sandage 1958). In the "normal" globular clusters the central star densities ρ_c (in $M_\odot \text{ pc}^{-3}$) lie in the range $\rho_c \sim 10^1 - 10^5$, whereas for the Palomar clusters $\rho_c \sim 1$ (Peterson and King 1975). The dwarf spheroidals have still lower densities near $\rho_c \sim 10^{-3}$; though by virtue of their larger linear diameters they have total masses comparable to the largest globular clusters (Hodge 1971). The dwarf spheroidals are thus extremely tenuous structures in comparison with the normal globular clusters, with the Palomar objects being intermediate.

(2) The available photometry of their individual stars by photometric systems sensitive to metallicity criteria (Hartwick and McClure 1974; Canterna 1975) indicates extremely low heavy-element abundance, up to 10 times lower than the classic metal-poor clusters M92 or M15.

(3) The CM diagrams obtained so far for these objects (Burbidge and Sandage 1958; Baade and Swope 1961; Hodge 1965; van Agt 1967; Swope 1967; Demers and Kunkel 1976) show unique features, e.g., predominantly red horizontal branches combined with steep yet moderately red giant branches, that are now interpreted as due to combinations of ages and abundances distinctly unlike those of any normal globular clusters (Hartwick and McClure 1974; Castellani 1975; Norris and Zinn 1975; Demarque and Hirshfeld 1975). It should be stressed that these CM anomalies are both more extreme and probably of different causes than the more well-known "second-parameter" problem found within the normal clusters. Variations in the color of the horizontal branch or the position and slope of the giant branch in the CM diagram which do not correspond exactly with cluster metallicity are now known to be quite widespread (including, for example, M13, M5, NGC 7006, NGC 362, NGC 288, M22, and others) within the normal clusters themselves, and recent discussions (Rood 1973; McClure and Norris 1974; Hesser, Hartwick, and McClure 1976) are leading to the conclusion that relatively minor variations in CNO abundances, helium abundance, or cluster age are capable of reproducing the observed variations. By contrast, interpretations of the dwarf spheroidals and Palomar clusters appear to require far more drastic differences in age or abundance (cf. the discussions by the authors cited).

(4) The variable stars present in the outlying systems have well-known peculiar properties. The mean periods of the RR Lyrae stars in some of them fall between the two Oosterhoff groups typifying the regular globular clusters, and the Population II cepheids differ markedly from the ones in normal clusters both in the period-frequency and period-luminosity relations (van Agt 1973; van den Bergh 1975; Norris and Zinn 1975; Demarque and Hirshfeld 1975). The various evolutionary interpretations for this situation are again discussed by the authors cited.

(5) The distribution in space of the outermost systems is nonisotropic. Kunkel and Demers (1975a, 1975b) and Lynden-Bell (1976) have recently pointed out that many of the objects concerned fall along a single great circle on the sky which transforms into one orbital plane (possibly even associated with the Magellanic Stream) about the galactic center when the objects are located in three dimensions. Some additional support for this picture is provided by several similarities between the characteristics of the dwarf spheroidals and the old stellar populations of the Magellanic Clouds themselves (e.g., van den Bergh 1975; Graham 1975). If this orbital plane hypothesis proves valid, then it would imply that several of the outermost objects have dynamically associated histories separate from the halo. The data involved are, of course, rudimentary as yet, and much more information on the exact distances and radial velocities of the individual objects will be needed to test the hypothesis in detail.

The outlying systems could legitimately be considered part of the galactic globular cluster system if their properties represented simply outward extensions of the properties of the inner, "normal" globular clusters. But the characteristics listed above may instead separate them discontinuously from the normal clusters. Within the inner cluster system ($r < 30$ kpc), no objects are known with such extremely low heavy-element content; and there is no outward trend for the normal clusters to become progressively more diffuse, to develop peculiar variables and anomalous CM diagrams, or to take up a nonisotropic space distribution. The combined evidence is thus extremely indicative that the distant clusters and dwarf spheroidal systems represent a somewhat different physical regime than the normal cluster system and have not formed or evolved in similar ways.

At least one exception to this overall picture is already known. We might now say that the "normal" cluster system fades out somewhere near $r \sim 40$ kpc and that all the objects beyond this are anomalous, were it not for the single object NGC 2419, which is an entirely normal, luminous metal-poor cluster at $r \approx 100$ kpc (Racine and Harris 1975). The reason that this uniquely interesting object lies so far beyond the limit of the regular cluster system (although its perigalacticon is within 30 kpc; see Racine and Harris) yet is so unlike all the other objects at that distance, remains unsolved.

We may ask conversely whether any "anomalous" clusters (i.e., any clusters sharing the five characteristics listed above) exist *within* the approximate 40-kpc radius of the normal cluster system. This may actually be the case but it is difficult to answer from the present meager data. The two best possible candidates with available CM diagrams are Pal 13 at $r = 25$ kpc, and NGC 7006 at $r = 32$ kpc. The former is the smallest known globular cluster, and is so sparse that it is hard to classify unambiguously. NGC 7006 does have an anomalous CM diagram for its metallicity type, but is otherwise a normal cluster, sharing none of the other characteristics of the outlying systems; it is luminous, very compact (Peterson and King 1975), does not appear to have peculiar variables, and has an abundance like that of an average metal-poor globular cluster (Canterna 1975; Hesser *et al.* 1976). Though it was originally thought to be connected with the more distant systems (Sandage and Wildey 1967), recent interpretations suggest that its red horizontal branch is due to enhanced nitrogen abundance (e.g., Hartwick and McClure 1972; Hartwick and Vanden Berg 1973). Lastly, a few other unstudied Palomar clusters exist at roughly similar distances ($r \sim 30$ kpc). For the time being these are included in Table VI as part of the cluster system, but with the knowledge that they should be investigated in detail before firm conclusions about their status can be reached.

In summary, the combined available data lead to the following, still tentative, picture for the structure of the outer halo.

(a) The normal cluster system, whose features were

described in Sec. VII-A,B, fades out almost entirely at $r \simeq 30\text{--}50$ kpc. One normal cluster (NGC 2419) is known which has penetrated to $r \sim 100$ kpc. (b) Beyond $r \simeq 40$ kpc the systematic properties of the Population II objects undergo a major change, into the five anomalous characteristics summarized above. In these respects the Palomar clusters bear certain resemblances to the dwarf spheroidal systems, though the latter objects represent the most extreme deviation from the properties of the inner halo clusters. (c) The spatial division between the normal (inner) and anomalous (outer) regions seems surprisingly clear. Certain clusters (Pal 13 or others) belonging to the anomalous group *may* exist within $r \simeq 40$ kpc, but the great majority lie well beyond the radius of the normal cluster system.

Interpretations of these data are still only guessed at, and indeed the various outlying objects may represent several different formation processes in themselves. Recent discussions by several authors (e.g., van den Bergh 1973; Castellani 1975; Norris and Zinn 1975; Demarque and Hirschfeld 1975) conclude that some of the objects may have formed much more recently than the initial collapse phase, or in regions with much less-enriched compositions, or both. Some others may have formed in a single orbital plane (e.g., under the stimulus of tidal interaction; see Kunkel and Demers 1975a, 1975b; Lynden-Bell 1976) quite separate from the protogalactic collapse phase in which the inner part of the halo is believed to have condensed. [In this sense the "normal" globular cluster system might now be defined as the group of *coeval* objects formed in the initial rapid collapse phase. Referring to the formation models of Larson (1975, 1976), it is then attractive to speculate that the apparent boundary $r \sim 40$ kpc may simply mark the size of the original protogalactic "cell" which participated in the collapse. In turn, the outlying systems may delineate a transition region between the halo proper and intergalactic space, where formation proceeded more gradually in a zone of much lower density and chemical enrichment (cf. also van den Bergh 1973).] Accurate assessments of which outlying objects do belong to the normal cluster system (in the sense of having formed along with it) must await much more comprehensive new data. Radial velocities, CM diagrams, and abundance studies need to be accumulated to determine the locations, orbital motions, and compositions of all the individual objects concerned.

Finally, we may return to the determination of $\varphi(r)$ for the outer region. Since the valid selection of clusters is so difficult here, the most reasonable approach appears to be to place upper and lower bounds on φ instead. An *upper* limit to φ may be set by blindly assuming all the Population II objects beyond $r = 40$ kpc to be part of the cluster system, regardless of any of their anomalous properties. The results are displayed in Table VI and Fig. 7. Ten objects are known with $r > 40$ kpc and $X < R_0$: Pal 1 in the 30–60-kpc shell; Draco, Sculptor, and Ursa Minor at 60–90 kpc; NGC 2419, Pal 3, and Pal 4 at

90–120 kpc; and Fornax, Leo I, and Leo II at 120–180 kpc. The result (small dots in Fig. 7) is that $\varphi(r)$ extends outward roughly as $\varphi \sim r^{-3}$ from the curve for the inner regions.

Taking the opposite extreme, we may set a firm *lower* limit to φ by rigorously excluding all the objects displaying any of the anomalous characteristics discussed previously. This leaves only NGC 2419 as the single clearly "normal" cluster in the four outer radial shells listed (large dots in Fig. 7). In this case, $\varphi(r)$ would fall off outward as $\varphi \sim r^{-4}$ or even more steeply if weight is given to the shells containing no clusters. [Both the radial placement and size of the shells are, of course, arbitrary, so that the three entries of $-\infty$ in Table VI are a consequence of the extremely small number of objects. If the four shells are combined, then the single point for NGC 2419 in Fig. 7 becomes $\log \varphi = -7.1$ at $\log r = 2.16$, and $\varphi(r)$ would be extrapolated roughly as r^{-4} again.]

Although the estimate for φ will be uncertain regardless of the initial assumptions (a statistical consequence of the small numbers of objects), the true shape of $\varphi(r)$ can be expected to be between the two extremes. Several of the anomalous objects are likely to be rejected as having too different evolutionary histories to be considered part of the normal cluster system, yet some may be maintained as members once more complete observational data are available. The dwarf spheroidals bear the least resemblance to the normal globular clusters and are therefore most likely to be excluded, while the Palomar clusters fall somewhat closer to the normal sequence. For the present, the $\varphi(r) \sim r^{-3.5}$ law established for the inner halo appears to be a satisfactory approximation for the outer halo as well.

D. The Projected Space Distribution

Another question of interest is how the cluster system would appear from a point distant in space, i.e., on the plane of the sky for a distant observer. Such information will be useful in comparing the structure of the cluster system with those in other galaxies. The projected distribution will be denoted as $\sigma(R)$ (clusters/kpc²), where R is now the distance from the galactic center projected in two dimensions.

The shape of σ may be derived either from integration of the three-dimensional distribution $\varphi(r)$, or straight from the observational data. The two methods are equivalent since the same data are used, but the latter is adopted here for directness. The best projection of the cluster distribution for this purpose is the YZ plane of Fig. 3, since in the other two projections (XZ , XY) the selection effects along the X axis would cause asymmetry in the observed distribution. Once again, only the clusters on the near side of the galactic center ($X < R_0$) are taken as the most nearly unbiased sample of the total system. Their distribution in the YZ plane is plotted and then doubled to compensate for the other half of the system.

TABLE VII. Projected density distribution.

R range (kpc)	$N(R)^a$	$\log \sigma(R)$ (kpc $^{-2}$)
0–1	34	1.03
1–2	19	0.30
2–3	18	0.06
3–4	6	-0.56
4–6	18	-0.54
6–8	10	-0.94
8–10	16	-0.85
10–12	8	-1.24
12–15	4	-1.80
15–20	4	-2.14
20–25	4	-2.25
25–30	2	-2.64
30–50	2:	-3.40

^a $N(R)$ equals the number of clusters with $X < R_0$ projected on the YZ plane in each R ring, doubled to compensate for the far half ($X > R_0$) of the cluster system.

The results are presented in Table VII and Fig. 9. Here, $R = (Y^2 + Z^2)^{1/2}$ is the projected distance from the center; $N(R)$ is the number of clusters with $X < R_0$ falling in each given ring, doubled; and $\sigma(R)$ is the corresponding surface density of clusters in each ring. The σ values, plotted in Fig. 9, are seen to fall off smoothly as $\sigma \sim R^{-2.5}$, as is expected from $\varphi \sim r^{-3.5}$.

It will be of great interest to determine whether the shape of the cluster distribution in our Galaxy, and hence the structure of the halo, is similar to those in other major galaxies. Although information is available for very few other galaxies, perhaps the next best studied cluster system in this respect is that in M87, the giant elliptical in Virgo. In M87, the density distribution of the globular clusters behaves as $\sigma \sim r^{-1.5} - r^{-2.0}$ (Racine 1968; Harris and Smith 1976), which is a noticeably flatter distribution than in the Galaxy. This may provide evidence that significant structural differences exist among the halos of large galaxies of different types, particularly if such variations are found in further studies of other galaxies.

VIII. THE MASS OF THE HALO

If the distribution of the globular clusters in space follows the mass distribution of the Population II stars in the halo as a whole, then we may use the cluster system to derive an estimate of M_h , the total mass contained in the halo. This procedure avoids introducing any particular theoretical model for the halo and assumes only that one type of halo object (the clusters) is a valid indicator of the halo in general.

From the smoothed plot of the mass density distribution $\rho(r)$ for the cluster system (Table VI), the overall mass contributed by the clusters in the solar neighborhood is $\rho_{\odot}(\text{clusters}) \simeq 1.4 \times 10^{-6} M_{\odot} \text{ pc}^{-3}$. Comparison of this with the local mass density of halo stars then gives the fraction of the halo mass contributed by the clusters. This latter quantity is still poorly known: Recent estimates of the local density of Population II stars range from $\rho_{\odot}(\text{halo}) \simeq 3 \times 10^{-5} - 10^{-3} M_{\odot} \text{ pc}^{-3}$ (e.g., Oort

1965; Bond 1970; Weistropp 1972, 1975; Innanen 1973; Schmidt 1975). If we adopt a value $\rho_{\odot}(\text{halo}) \simeq 5 \times 10^{-4} M_{\odot} \text{ pc}^{-3}$ following Weistropp (1975) or Schmidt (1975), then $\rho(\text{halo})/\rho(\text{clusters}) \simeq 350$. Now, since there are ~ 200 globular clusters in the Galaxy (see Sec. VI) and the mean mass for the individual clusters in our sample is $\sim 2 \times 10^5 M_{\odot}$ for a mass-to-light ratio of 1.5, then the total mass contained in the cluster system is $M_{\text{cl}} \sim 4 \times 10^7 M_{\odot}$. Finally, multiplying this by the ratio $M_h/M_{\text{cl}} = 350$ yields $M_h \simeq 1.4 \times 10^{10} M_{\odot}$, which is $\sim 10\%-20\%$ of the mass of the disk and nucleus (Schmidt 1965; Innanen 1973). Three-quarters of this mass lies within a sphere of radius $r = 10$ kpc.

This result for M_h might easily be in error by a factor of 10, because of the currently large observational uncertainties in $\rho_{\odot}(\text{halo})$. [Interestingly, M_h is independent of the assumed mass-to-light ratio for the globular clusters, since M/L cancels out when $\rho_{\odot}(\text{halo})/\rho_{\odot}(\text{clusters})$ is multiplied by M_{cl} .] Nevertheless, taken at face value the result provides support for the view that the “normal” halo (i.e., Population II stars and clusters) is not massive enough by itself to stabilize the disk. The “massive halo” models described recently (Ostriker and Peebles 1973; Ostriker *et al.* 1974) require the halo to be $\sim 50\%$ or more of the disk mass, and also generally assume a much flatter density gradient than the $\varphi \sim r^{-3.5}$ law (since less centrally concentrated halos are relatively more efficient at stabilization). The M_h estimate from the globular cluster system is therefore consistent with the view that any existing massive halo within our own Galaxy should be in the form of nonluminous matter (degenerate stars, black holes, etc.) whose density distribution $\varphi(r)$ is different from the ordinary Population II halo.

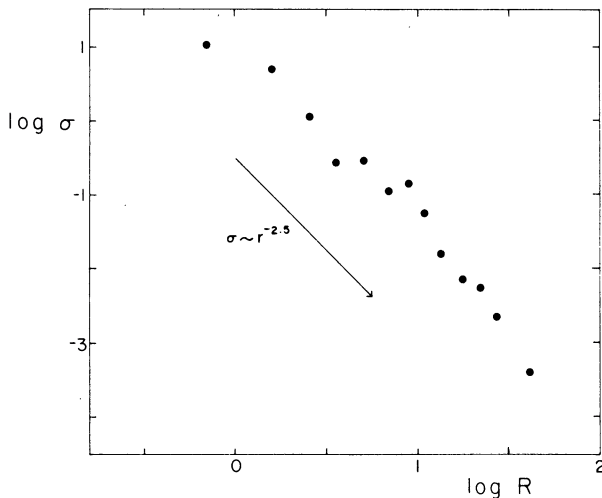


FIG. 9. The projected (two-dimensional) space distribution $\sigma(R)$ of the cluster system, as listed in Table VII. Here σ equals the number of clusters/kpc 2 as projected on the YZ plane, as a function of the projected distance R from the center, where $R = (Y^2 + Z^2)^{1/2}$. The expected power law distribution $\sigma \sim R^{-2.5}$ is drawn in.

ACKNOWLEDGMENTS

For many helpful comments on this material and on the manuscript, I am sincerely indebted to Dr. G. L. H. Harris, Dr. J. E. Hesser, and Dr. R. D. McClure. This work was financially supported through the National Research Council of Canada and Yale University Observatory.

REFERENCES

- Aannestad, P. A., and Purcell, E. M. (1973). *Ann. Rev. Astron. Astrophys.* **11**, 309.
- Alcaino, G. (1971a). *Astron. Astrophys.* **13**, 399.
- Alcaino, G. (1971b). *Astron. Astrophys.* **15**, 360.
- Alcaino, G. (1972). *Astron. Astrophys.* **16**, 220.
- Alcaino, G. (1974a). *Astron. Astrophys. Suppl.* **13**, 55.
- Alcaino, G. (1974b). *Astron. Astrophys. Suppl.* **18**, 9.
- Alcaino, G., and Contreras, C. (1971). *Astron. Astrophys.* **11**, 14.
- Alter, G., Balazs, B., and Ruprecht, J. (1970). *Catalogue of Star Clusters and Associations* (Akademiai Kiado, Budapest), 2nd ed.
- Arp, H. C. (1955). *Astron. J.* **60**, 317.
- Arp, H. C. (1962). *Astrophys. J.* **135**, 311.
- Arp, H. C. (1965a). In *Galactic Structure*, edited by A. Blaauw and M. Schmidt (Univ. Chicago P., Chicago), Ch. 19, p. 401.
- Arp, H. C. (1965b). *Astrophys. J.* **141**, 43.
- Arp, H. C., and Hartwick, F. D. A. (1971). *Astrophys. J.* **167**, 499.
- Arp, H. C., and Melbourne, W. G. (1959). *Astron. J.* **64**, 28.
- Baade, W. (1958). In *Stellar Populations*, edited by D. J. K. O'Connell (Interscience, New York), p. 303.
- Baade, W., and Swope, H. (1961). *Astron. J.* **66**, 300.
- Balona, L. A., and Feast, M. W. (1974). *Mon. Not. R. Astron. Soc.* **167**, 621.
- Barbon, R. (1965). *Asiago Contrib.* No. 175.
- Barnes, S. A. (1968). *Astron. J.* **73**, 579.
- Bond, H. E. (1970). *Astrophys. J. Suppl.* **22**, 117.
- Breger, M., and Bregman, J. N. (1975). *Astrophys. J.* **200**, 343.
- Burbidge, E. M., and Sandage, A. R. (1958). *Astrophys. J.* **127**, 527.
- Burstein, D., and McDonald, L. H. (1975). *Astron. J.* **80**, 17.
- Cannon, R. D. (1974). *Mon. Not. R. Astron. Soc.* **167**, 551.
- Cannon, R. D., and Stobie, R. S. (1973). *Mon. Not. R. Astron. Soc.* **163**, 227.
- Canterna, R. (1975). *Astrophys. J. Lett.* **200**, L63.
- Castellani, V. (1975). *Mon. Not. R. Astron. Soc.* **172**, 59P.
- Christy, R. F. (1966). *Astrophys. J.* **144**, 108.
- Ciatti, F., Rosino, L., and Sussi, M. G. (1965). *Padova Comm. No. 44*.
- Crampton, D., and Georgelin, Y. M. (1975). *Astron. Astrophys.* **40**, 317.
- Cuffey, J. (1961). *Astron. J.* **66**, 71.
- Cuffey, J. (1965). *Astron. J.* **70**, 232.
- Demarque, P., and Hirshfeld, A. (1975). *Astrophys. J.* **202**, 346.
- Demarque, P., and McClure, R. D. (1976). Submitted.
- Demers, S., and Kunkel, W. (1976). Preprint.
- Dickens, R. J. (1970). *Astrophys. J. Suppl.* **22**, 249.
- Dickens, R. J. (1972a). *Mon. Not. R. Astron. Soc.* **157**, 281.
- Dickens, R. J. (1972b). *Mon. Not. R. Astron. Soc.* **157**, 299.
- Dickens, R. J., and Rolland, A. (1972). *Mon. Not. R. Astron. Soc.* **160**, 37.
- Dickens, R. J., and Saunders, J. (1965). *R. Obs. Bull.* No. 101.
- Eggen, O. J. (1972). *Astrophys. J.* **172**, 639.
- Eggen, O. J., Lynden-Bell, D., and Sandage, A. (1962). *Astrophys. J.* **136**, 748.
- Fernie, J. D. (1962). *Astron. J.* **67**, 769.
- Fourcade, C. R., Laborde, J. R., and Arias, J. C. (1974). *Astron. Astrophys. Suppl.* **18**, 1.
- Graham, J. A. (1973). In *Variable Stars in Globular Clusters and in Related Systems*, IAU Colloq. No. 21, edited by J. D. Fernie (Reidel, Dordrecht), p. 120.
- Graham, J. A. (1975). *Publ. Astron. Soc. Pac.* **87**, 641.
- Harris, W. E. (1974). Ph.D. thesis, Univ. Toronto.
- Harris, W. E. (1975). *Astrophys. J. Suppl.* **29**, 397.
- Harris, W. E., and Racine, R. (1973). *Astron. J.* **78**, 242.
- Harris, W. E., and Racine, R. (1974). *Astron. J.* **79**, 472.
- Harris, W. E., Racine, R., and de Roux, J. (1976). *Astrophys. J. Suppl.* **31**, 13.
- Harris, W. E., and Smith, M. G. (1976). *Astrophys. J.* **207**, 1036.
- Harris, W. E., and van den Bergh, S. (1974). *Astron. J.* **79**, 31.
- Hartwick, F. D. A. (1975). *Publ. Astron. Soc. Pac.* **87**, 77.
- Hartwick, F. D. A., and Hesser, J. E. (1972). *Astrophys. J.* **175**, 77.
- Hartwick, F. D. A., and Hesser, J. E. (1973). *Astrophys. J.* **186**, 1171.
- Hartwick, F. D. A., and Hesser, J. E. (1974). *Astrophys. J. Lett.* **194**, L129.
- Hartwick, F. D. A., and McClure, R. D. (1972). *Astrophys. J. Lett.* **176**, L57.
- Hartwick, F. D. A., and McClure, R. D. (1974). *Astrophys. J.* **193**, 321.
- Hartwick, F. D. A., and Sandage, A. (1968). *Astrophys. J.* **153**, 715.
- Hartwick, F. D. A., and Vanden Berg, D. A. (1973). *Publ. Astron. Soc. Pac.* **85**, 355.
- Heck, A. (1973). *Astron. Astrophys.* **24**, 313.
- Hemenway, M. K. (1975). *Astron. J.* **80**, 199.
- Herbst, W. (1975). *Astron. J.* **80**, 498.
- Hesser, J. E., and Hartwick, F. D. A. (1976a). *Astrophys. J.* **203**, 97.
- Hesser, J. E., and Hartwick, F. D. A. (1976b). *Astrophys. J.* **203**, 113.
- Hesser, J. E., Hartwick, F. D. A., and McClure, R. D. (1976). Submitted.
- Hodge, P. W. (1971). *Ann. Rev. Astron. Astrophys.* **9**, 35.
- Iben, I. (1971). *Publ. Astron. Soc. Pac.* **83**, 687.
- Illingworth, G. (1975). In *Dynamics of Stellar Systems*, IAU Symp. No. 69, edited by A. Hayli (Reidel, Dordrecht), p. 151.
- Illingworth, G., and Freeman, K. C. (1974). *Astrophys. J. Lett.* **188**, L83.
- Innanen, K. A. (1973). *Astrophys. Space Sci.* **22**, 393.
- Kinman, T. D. (1958). *Mon. Not. Astron. Soc. S. Africa* **17**, 19.
- Kinman, T. D. (1959a). *Mon. Not. R. Astron. Soc.* **119**, 538.
- Kinman, T. D. (1959b). *Mon. Not. R. Astron. Soc.* **119**, 499.
- Kinman, T. D., and Rosino, L. (1962). *Publ. Astron. Soc. Pac.* **74**, 499.
- Kogan, C. S., Wehlau, A., and Demers, S. (1974). *Astron. J.* **79**, 387.
- Kron, G. E., and Mayall, N. U. (1960). *Astron. J.* **65**, 581.
- Kukarkin, B. V. (1971). *Soviet A. J.* **15**, 89.
- Kukarkin, B. B. (1974). *The Globular Star Clusters* (Sternberg State Astron. Inst., Nauka, Moscow).
- Kunkel, W., and Demers, S. (1975a). Paper delivered at tercentenary Symposium of Royal Greenwich Observatory.
- Kunkel, W., and Demers, S. (1975b). *Bull. Am. Astron. Soc.* **7**, 550.

- Larson, R. B. (1974). Mon. Not. R. Astron. Soc. **145**, 405.
- Larson, R. B. (1975). In *Dynamics of Stellar Systems*, IAU Symp. No. 69, edited by A. Hayli (Reidel, Dordrecht), p. 247.
- Larson, R. B. (1976). Mon. Not. R. Astron. Soc. **176**, 31.
- Liller, M. H., and Liller, W. (1975). Bull. Am. Astron. Soc. **7**, 536.
- Lynden-Bell, D. (1976). Mon. Not. R. Astron. Soc. **174**, 695.
- Mayall, N. U. (1946). Astrophys. J. **104**, 290.
- McClure, R. D., and Crawford, D. L. (1971). Astron. J. **76**, 31.
- McClure, R. D., and Norris, J. (1974). Astrophys. J. **193**, 139.
- Menzies, J. W. (1967). Ph.D. thesis, Aust. Natl. U.
- Menzies, J. W. (1972). Mon. Not. R. Astron. Soc. **156**, 207.
- Menzies, J. W. (1974a). Mon. Not. R. Astron. Soc. **168**, 177.
- Menzies, J. W. (1974b). Mon. Not. R. Astron. Soc. **169**, 79.
- Morgan, W. W. (1956). Publ. Astron. Soc. Pac. **68**, 509.
- Morgan, W. W. (1959). Astron. J. **64**, 432.
- Norris, J., and Zinn, R. (1975). Astrophys. J. **202**, 335.
- Oort, J. H. (1965). In *Galactic Structure*, edited by A. Blaauw and M. Schmidt (Univ. Chicago P., Chicago), Ch. 21, p. 455.
- Oort, J. H., and Plaut, L. (1975). Astron. Astrophys. **41**, 71.
- Ostriker, J. P., and Peebles, P. J. E. (1973). Astrophys. J. **186**, 467.
- Ostriker, J. P., Peebles, P. J. E., and Yahil, A. (1974). Astrophys. J. Lett. **193**, L1.
- Peterson, C. J., and King, I. R. (1975). Astron. J. **80**, 427.
- Philip, A. G. D. (1974). Astrophys. J. **190**, 573.
- Philip, A. G. D., and Tifft, L. (1971). Astron. J. **76**, 567.
- Racine, R. (1968). J. R. Astron. Soc. Can. **62**, 367.
- Racine, R. (1971). Astron. J. **76**, 331.
- Racine, R. (1973). Astron. J. **78**, 180.
- Racine, R. (1974). Unpublished.
- Racine, R. (1976). Preprint.
- Racine, R., and Harris, W. E. (1975). Astrophys. J. **196**, 413.
- Rybicki, G., Lecar, M., and Schaefer, M. (1974). Bull. Am. Astron. Soc. **6**, 453.
- Sandage, A. (1969). Astrophys. J. **157**, 515.
- Sandage, A. (1970). Astrophys. J. **162**, 841.
- Sandage, A. (1972). Astrophys. J. **178**, 1.
- Sandage, A. (1973). Astrophys. J. **183**, 711.
- Sandage, A., and Katem, B. (1968). Astrophys. J. **153**, 569.
- Sandage, A., and Smith, L. L. (1966). Astrophys. J. **144**, 886.
- Sandage, A., and Walker, M. F. (1955). Astron. J. **60**, 230.
- Sandage, A., and Wallerstein, G. (1960). Astrophys. J. **131**, 598.
- Sandage, A., and Wildey, R. (1967). Astrophys. J. **150**, 469.
- Sawyer Hogg, H. (1959). *Handbuch der Physik*, edited by S. Flugge (Springer-Verlag, Berlin), Vol. 53, p. 129.
- Sawyer Hogg, H. (1973). Publ. David Dunlap Obs. **3**, No. 6.
- Schmidt, M. (1965). In *Galactic Structure*, edited by A. Blaauw and M. Schmidt (Univ. Chicago P., Chicago), Ch. 22, p. 513.
- Schmidt, M. (1975). Astrophys. J. **202**, 22.
- Shapley, H. (1918). Astrophys. J. **48**, 89.
- Shapley, H. (1930). In *Star Clusters* (McGraw-Hill, New York), Ch. XI.
- Stobie, R. S. (1971). Astrophys. J. **168**, 381.
- Stetson, P., and Harris, W. E. (1976). In preparation.
- Swope, H. (1967). Publ. Astron. Soc. Pac. **79**, 439.
- Thackeray, A. D. (1972). Q. J. R. Astron. Soc. **13**, 243.
- Toomre, A. (1972). Q. J. R. Astron. Soc. **13**, 241.
- van Agt, S. (1967). Bull. Astron. Inst. Neth. **19**, 275.
- van Agt, S. (1973). In *Variable Stars in Globular Clusters and in Related Systems*, IAU Colloq. No. 21, edited by J. D. Fermie (Reidel, Dordrecht), p. 35.
- van Albada, T. S., and Baker, N. H. (1973). Astrophys. J. **185**, 477.
- van den Bergh, S. (1967a). Astron. J. **72**, 70.
- van den Bergh, S. (1967b). J. R. Astron. Soc. Can. **61**, 179.
- van den Bergh, S. (1971). Astron. J. **76**, 1082.
- van den Bergh, S. (1973). Astron. Astrophys. **28**, 469.
- van den Bergh, S. (1974). Astrophys. J. Lett. **188**, L9.
- van den Bergh, S. (1975). Ann. Rev. Astron. Astrophys. **13**, 217.
- van Herk, G. (1965). Bull. Astron. Inst. Neth. **18**, 71.
- Walker, M. F., Pike, C. D., and McGee, J. D. (1976). Mon. Not. R. Astron. Soc. **175**, 525.
- Weistroop, D. (1972). Astron. J. **77**, 366.
- Weistroop, D. (1975). Astron. J. **80**, 303.
- Woltjer, L. (1975). Astron. Astrophys. **42**, 109.
- Woolley, R. v. d. R., and Savage, A. (1971). R. Obs. Bull. No. 170.